SPECIAL REPORT CR-FCDD-AMV-19-01

QUASI-STEADY MANEUVERING OF PENDANT DUAL LIFT SYSTEMS

Luigi S. Cicolani
San Jose State University Research Foundation

Prepared for:

Aviation Development Directorate – Ames
Combat Capabilities Development Command
Aviation & Missile Center

September 2019

DESTRUCTION NOTICE

FOR CLASSIFIED DOCUMENTS, FOLLOW THE PROCEDURES IN DoD 5200.22-M, INDUSTRIAL SECURITY MANUAL, SECTION II-19 OR DoD 5200.1-R, INFORMATION SECURITY PROGRAM REGULATION, CHAPTER IX. FOR UNCLASSIFIED, LIMITED DOCUMENTS, DESTROY BY ANY METHOD THAT WILL PREVENT DISCLOSURE OF CONTENTS OR RECONSTRUCTION OF THE DOCUMENT.

DISCLAIMER

THE FINDINGS IN THIS REPORT ARE NOT TO BE CONSTRUED AS AN OFFICIAL DEPARTMENT OF THE ARMY POSITION UNLESS SO DESIGNATED BY OTHER AUTHORIZED DOCUMENTS.

TRADE NAMES

USE OF TRADE NAMES OR MANUFACTURERS IN THIS REPORT DOES NOT CONSTITUTE AN OFFICIAL ENDORSEMENT OR APPROVAL OF THE USE OF SUCH COMMERCIAL HARDWARE OR SOFTWARE.

REPORT DOCUMENTATION PAGE			Form Approved OMB No. 0704-0188
The public reporting burden for this collection of information is estimated to average 1 hour per response, including the time for reviewing instructions, searching existing data sources, gathering and maintaining the data needed, and completing and reviewing the collection of information. Send comments regarding this burden estimate or any other aspect of this collection of information, including suggestions for reducing the burden, to the Department of Defense, Executive Service Directorate (0704-0188). Respondents should be aware that notwithstanding any other provision of law, no person shall be subject to any penalty for failing to comply with a collection of information if it does not display a currently valid OMB control number.			
PLEASE DO NOT RETURN YOUR FORM TO THE ABOVE ORGANIZATION.			
1. REPORT DATE *(DD-MM-YYYY)* September 2019	**2. REPORT TYPE** Final		**3. DATES COVERED** *(From - To)*
4. TITLE AND SUBTITLE Quasi-Steady Maneuvering of Pendant Dual Lift Systems			**5a. CONTRACT NUMBER** **5b. GRANT NUMBER** **5c. PROGRAM ELEMENT NUMBER**
6. AUTHOR(S) Luigi S. Cicolani			**5d. PROJECT NUMBER** **5e. TASK NUMBER** **5f. WORK UNIT NUMBER**
7. PERFORMING ORGANIZATION NAME(S) AND ADDRESS(ES) Commander, U.S. Army Combat Capabilities Development Command ATTN: FCDD-AMV-A Redstone Arsenal, AL 35898-5000			**8. PERFORMING ORGANIZATION REPORT NUMBER** SR-CR-FCDD-AMV-19-01
9. SPONSORING/MONITORING AGENCY NAME(S) AND ADDRESS(ES)			**10. SPONSOR/MONITOR'S ACRONYM(S)** **11. SPONSOR/MONITOR'S REPORT NUMBER(S)**
12. DISTRIBUTION/AVAILABILITY STATEMENT Distribution Statement A: Approved for public release; distribution is unlimited.			
13. SUPPLEMENTARY NOTES			
14. ABSTRACT The US army flight research group at Moffett Field (CCDC AvMC ADD-A) undertook a dual lift project in which the load is carried in a pendant two-cable suspension. Work on simulation, feedback control, wind tunnel testing and a flight test with two RMAX helicopters has previously been published. This report analyses configuration management of the system to maintain the prescribed loading ratio for the two helicopters in general quasi-steady maneuvering flight. For equal cable lengths, equal loading is obtained by maintaining the hook-to-hook line segment perpendicular to the total load to be supported by the helicopter. The system can be flown with any formation angle. It was found that the side-by-side formation had general advantages in terms of simplicity of the required configuration management activity and insensitivity to load drag. Sensitivities of the cable tensions to configuration variables indicate that cable tensions are readily controlled by adjusting the vertical position of one helicopter relative to the other and that this sensitivity is nearly invariant with airspeed, formation angle and maneuvering. A study of a system of two UH-60s indicated that load drag and airframe aerodynamics have significant effects on helicopter thrust and attitude requirements in forward flight, depending on formation angle.			
15. SUBJECT TERMS dual lift systems, pendant dual lift system, configuration management, feedforward control, system maneuvering, formation angle, helicopter thrust and attitude requirements, load equalization, sensitivities			

16. SECURITY CLASSIFICATION OF:			**17. LIMITATION OF ABSTRACT**	**18. NUMBER OF PAGES**	**19a. NAME OF RESPONSIBLE PERSON**
a. REPORT	**b. ABSTRACT**	**c. THIS PAGE**			**19b. TELEPHONE NUMBER** *(Include area code)*
UNCLASSIFIED	UNCLASSIFIED	UNCLASSIFIED	SAR	43	

SUMMARY

The US army flight research group at Moffett Field (CCDC AvMC ADD-A) undertook a dual lift project in which the load is carried in a pendant two-cable suspension. Work has previously been published on simulation, feedback control, wind tunnel testing and a flight test with two RMAX helicopters. As part of that effort, this report analyses configuration management of the system to maintain the prescribed loading ratio for the two helicopters (usually equal loading for twin helicopters) in general quasi-steady maneuvering flight. The configuration can be managed by adjusting the vertical position of one helicopter relative to the other as required to execute maneuvers such as accelerations and turns. For equal cable lengths, equal loading is obtained by maintaining the hook-to-hook line segment perpendicular to the total load to be supported by the helicopters (sum of load weight, aerodynamics, and acceleration). The system can be flown with any formation angle relative to the flight path; that is, the helicopters can be in-line or side-by-side or anywhere in between. It was found that the side-by-side formation had general advantages in terms of simplicity of the required configuration management activity and insensitivity to load drag, but in a piloted system the pilots are tilted in roll. The in-line formation eliminates that problem for a piloted system but requires more configuration activity, and accuracy is sensitive to errors in estimating load drag. Sensitivities of the cable tensions to configuration variables indicate that cable tensions are readily controlled through the vertical position of the trail helicopter and that this sensitivity is nearly invariant with airspeed, formation angle and maneuvering. Helicopter thrust and attitude requirements are also studied for a system of two UH-60s carrying a high drag load. It was found that load drag and airframe aerodynamics have significant effects on helicopter attitude and thrust requirements in forward flight, depending on formation angle.

Configuration management can be implemented as a feed-forward element of a controller in a fully automatic system, or in an automated trail helicopter following a manned lead helicopter, or as a flight director in a fully manual system.

TABLE OF CONTENTS

LIST OF FIGURES

LIST OF TABLES

NOTATION AND SYMBOLS

Physical vectors without reference to any axes are given in boldface. Vectors given by their components in an axis frame are given in lightface with a subscript to indicate the axes. The subscript can be any of N (inertial axes), h (level heading axes), p (path axes), T (axes attached to the plane of the triangle formed by the pendant cables) or b (standard helicopter body axes; b1, b2 distinguish between helicopters 1 and 2 where necessary).

Local vertical axes with x in the direction of North (North, East, Down axes) are taken as inertial axes. Level heading axes are local vertical axes with x aligned with the heading of the flight path. In hover and vertical flight, the flight path heading is taken as that of the helicopter. Path axes are defined in forward flight with x aligned with the velocity vector, y perpendicular to the velocity vector in the horizontal plane and z perpendicular to the velocity vector in the vertical plane pointing downward. Triangle axes are defined with x along the hook-to-hook line segment, z perpendicular to that in the plane of the triangle and pointing downward, and y perpendicular to the plane of the triangle. All are right-handed axes.

a, aL	helicopter and load accelerations
D, L	Load drag and lift
$E_i(.)$	transformations for single axis rotations, i = 1,2,3
FA, FAL	helicopter and load aerodynamic forces
Fhk	Hook force on helicopter
FL, FL	apparent Load vector and magnitude
g, g	gravity vector and magnitude, 32.17 ft/sec2
h1,h2	altitude of helicopters 1 and 2
it,jt,kt	unit axes vectors for triangle axes
ih, jh, kh	unit axes vectors for level heading axes
ip, jp, kp	unit axes vectors for path axes
m	helicopter mass
k	unit local vertical (down) direction vector
ks	unit vertical stability axis (direction of lift)
L12	distance between hooks, ft
r21	hook to hook line segment, ft
T, T	helicopter thrust vector and magnitude
T_{hb}	Transformation from helicopter body axes to level heading axes
T_{Th}	Transformation from level heading axes to triangle axes
ul	unit direction vector of **FL**
ulx,y,z	components of **ul** in level heading axes
W, WL	helicopter weight, load weight. W1, W2 distinguishes between helicopters, lbs
rhs	right hand side of helicopter force balance equation, lbs
α	angle of attack, also noted as aoa, deg
ε_L	angle between **FL** and **kt,** deg
ϕ_{13}, θ_{13}	cable 1 pitch and roll angles relative to level heading axes, deg
ϕ_{23}, θ_{23}	cable 2 pitch and roll angles relative to level heading axes, deg

$\Delta\phi_{13}$, $\Delta\theta_{13}$	cable 1 roll and pitch angles relative to helicopter 1 body axes, deg
$\Delta\phi_{23}$, $\Delta\theta_{23}$	cable 2 roll and pitch angles relative to helicopter 2 body axes, deg
ζ	cable tension ratio, $\tau1/\tau2$
ϕ, θ	helicopter roll and pitch angles. $\phi1$, $\phi2$, etc. distinguish between HC's, deg
φ	roll angle representing lateral acceleration relative to load weight
ϕ_T, θ_T, ψ_T	triangle roll and pitch angles, formation angle, deg
θ_D, θ_L	angles representing load drag and lift relative to load weight
γ, ψ_V	flight path angle and velocity heading on a reference trajectory, deg
$\xi1$, $\xi2$	angles partitioning the separation angle between cables, deg
σ	separation angle between cables at the triangle vertex, deg
Σ	auxiliary angle, deg
$\tau1$,$\tau2$	tensions, cables 1, 2, lbs
$\Delta\tau$	cable tension difference, $\tau1$-$\tau2$, lbs

Abbreviations and Acronyms

ADD-A	Aviation Development Directorate – Ames
AvMC	Aviation & Missile Center
aoa	angle of attack, also noted as α, deg
CCDC	Combat Capabilities Development Command
HC	helicopter
HC1, HC2	enumeration of the two helicopters. HC1 leads the configuration.

1. INTRODUCTION

The use of two or more helicopters to carry a heavy load was proposed in the 1950's. Vertol conducted a feasibility study among various ways to connect the helicopters and load that pointed to the spreader bar dual lift configuration for further study [1]. Later, Sikorsky conducted a 1.2 hr flight test of this configuration using two CH54 helicopters carrying a 20 ton load [2]. High pilot workload was required to stabilize the system in hover and excessive workload was required to transition to forward flight. This pointed to the need for automatic stabilization and control assistance at the system level. Several private operators are also known to have tried twin lift in this period and [3] notes that twin lift operations were conducted in the USSR although details are unknown. The relative benefits of twin lift or multi-lift vs a single heavy lift helicopter are reviewed in [3] and [4]. The tradeoff is between twin lift using available helicopters vs calling in a helicopter with greater lift capability for the occasional heavy load, or between using twin lift to extend the lift capability of the existing military fleet vs developing a few heavy lift helicopters to carry infrequent high-weight loads at dispersed locations. These considerations concern full-scale manned military and civil operations. Similar considerations may apply to operators of small-scale unmanned rotorcraft. It may be noted that neither twin lift nor the heavy lift helicopter have come into being since the Joint Heavy Lift program of the 1970's.

Possible configurations using two helicopters are shown in Fig. 1. Analysis of the spreader bar dual lift system for configuration management [5], equations of motion [6], [7], [8], and control [9],[10], [11] are found in the literature. In the past there was little interest in the pendant configuration for manned flight owing to the uncomfortable steady state helicopter roll required in the side-by-side formation. However, the pendant configuration is readily extended to three or more helicopters with cables connecting each helicopter to the load. Recent studies have adopted its use for small-scale rotorcraft [12], [13] and for full-scale helicopters [14], [15]. References 12 and13 report a successful flight test using three small-scale helicopters carrying 9 lbs and the associated control methodology for autonomous multi-lift systems. References 14 and 15 consider a system with four UH-60 helicopters with cables connected to the corners of a cargo container, and methods of controlling the trajectory and attitude of the load.

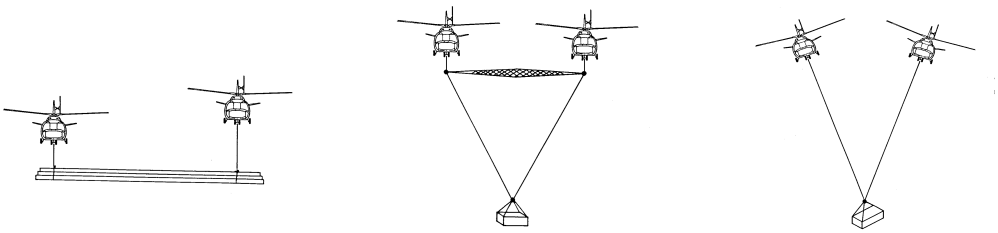

(a) long load (b) spreader bar (c) pendant suspension

Figure 1. Dual lift arrangements

The Army's Aviation Development Directorate at Moffett Field, CA. (CCDC AvMC ADD-A) engaged in a project in which the load is carried in the pendant two-cable suspension. Work has been done in simulation, control development and wind tunnel testing [16], [17] and a flight test

with two autonomous RMAX helicopters has been successfully carried out [18], [19]. The top level of the dual lift system control will regulate helicopter separation, formation angle and cable tensions during a mission. Control of separation and formation angle is relatively routine while control of cable tensions to maintain equal load distribution (or a prescribed load-sharing ratio) requires adjustment of the relative height of the two helicopters depending on configuration parameters, formation angle, maneuvering and load aerodynamics. The present report analyses management of the system configuration to maintain the prescribed loading ratio under general flight conditions.

Section 2 considers force balance at the load attachment point from which the configuration management requirements for general configuration parameter values (formation angle, equal or unequal loading, equal or unequal cable lengths, cable separation angle, load weight and drag) are derived. Results are given for a reference mission profile within the flight envelope of full-scale helicopters. The effects of formation angle on the required configuration management activity are reviewed. Control sensitivities for cable tensions are also studied. Section 3 considers trim requirements for the helicopters (thrust and attitude) with results along the reference mission for a system with two UH-60 helicopters. The effects of formation angle are reviewed.

2. CONFIGURATION MANAGEMENT DURING GENERAL QUASI-STEADY MANEUVERING

Quasi-steady flight refers to any static equilibrium flight condition or flight in which acceleration changes much more slowly than the system can change acceleration, including steady turns, turn entries and exits, speed changes, and speed rate changes. The analysis follows that previously given for the spreader bar dual lift configuration in [5].

Figure 2 shows the pendant triangle formed by the suspension cables (Fig. 2a) and the system formation angle (Fig. 2b).

Points 1, 2, 3 in Fig. 2(a) are the hooks of the lead and trail helicopters and the attachment point of the load, respectively. Assuming the cables are straight lines, then they define a plane to which an axis frame can be attached (triangle axes), {**it, jt, kt**}, where **it** is along the hook-to-hook line segment, **r21**, (directed from point 2 to point 1) and **kt** is the downward perpendicular to that in the plane of the triangle and **jt** is perpendicular to the plane to form a right-handed system. The cable separation angle is denoted σ, and can be divided into $\xi 1$, $\xi 2$ as shown. The formation angle, ψ_T, is the heading of the hook-to-hook line, **r21,** relative to the direction of flight (Fig. 2(b)).

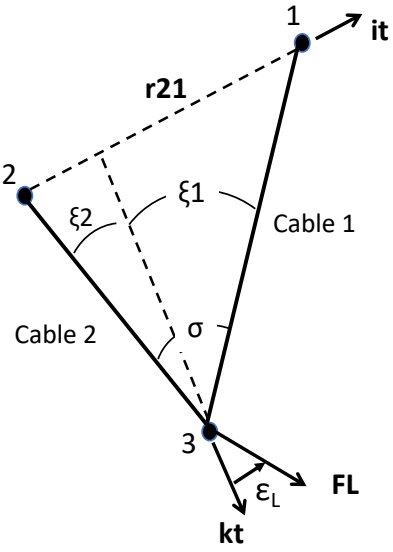

(a) Pendant triangle

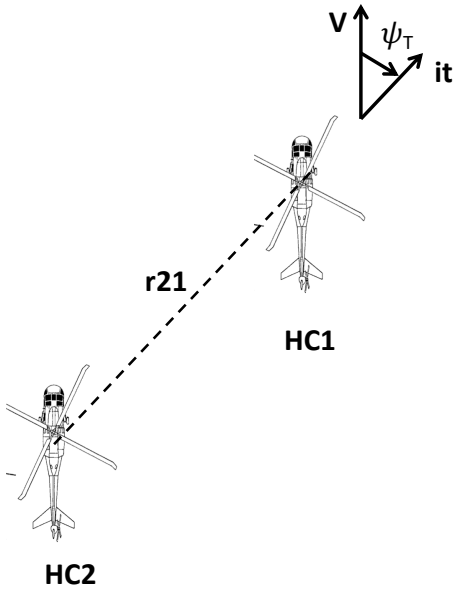

(b) formation angle

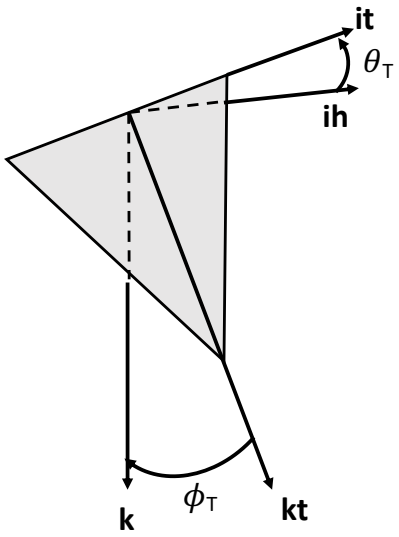

(c) triangle attitude angles

Figure 2. Pendant dual lift system

2.1 Force Balance at the Load Attachment. The load suspended by the pendant applies the apparent load, **FL**, to be carried by the helicopters

$$\mathbf{FL} = \mathbf{WL} + \mathbf{FAL} - m_L * \mathbf{aL} \tag{1a}$$

where all terms (load weight, aerodynamics and acceleration) are physical vectors (written in bold). Path axes, {**ip**, **jp**, **kp**} can be introduced to describe the load acceleration in more detail, where **ip** is along the velocity vector (path tangent), **kp** is the downward perpendicular to **ip** in the vertical plane and **jp** is lateral to **ip** in the horizontal plane. After dividing by load weight and separating into components, the apparent load is:

$$\frac{\mathbf{FL}}{\mathrm{WL}} = \mathbf{k} + \left(\frac{\dot{\mathrm{V}}}{g} + \tan\theta_D \right) \mathbf{ip} - \tan\varphi\ \mathbf{jp} - \frac{\mathrm{V}\dot{\gamma}}{g}\mathbf{kp} - \tan\theta_{\mathrm{L}}\mathbf{ks} \tag{1b}$$

where

$$\tan\theta_{\mathrm{D}} = \frac{\mathrm{D}}{\mathrm{WL}}$$

$$\tan\theta_{\mathrm{L}} = \frac{\mathrm{L}}{\mathrm{WL}}$$

$$\tan\varphi = \frac{\mathrm{V}\dot{\psi}}{\mathrm{WL}}$$

The major terms to consider are the weight along the local vertical, **k,** speed rate and drag along **ip**, turn acceleration along **jp** and lift along **ks**, where **ks** is perpendicular to velocity in the x-z plane of the load body axes. Typical speed rates are limited to about 0.1g for helicopter operations, the drag angle can reach 45 deg (1 g) depending on airspeed and load drag characteristics, and turn accelerations might reach 0.5g. Load lift may be present, often as negative lift of the nose-down trailing load, depending on airspeed, but is usually much smaller than load weight or drag for typical bluff body loads. Equation 1 indicates that load drag is equivalent to speed rate and, for straight and level flight, load lift is equivalent to weight. The aerodynamics of the load hanging below the pendant can vary continually due to rotational and pendulum oscillations of the load. These variations are neglected in the present study of quasi-steady maneuvering in favor of the mean steady state aerodynamics. During a mission, **FL** varies from parallel to the local vertical in hover to significant offsets from the vertical principally due to load drag and turn accelerations and this will require managing the relative positions of the two helicopters to maintain equal loading or a prescribed loading ratio, as discussed next.

Force balance requires that the apparent load lie in the plane of the triangle. In that case, simple expressions can be given for the two cable tensions in terms of the cable separation angle, σ, its parts, $\xi 1$, $\xi 2$, (angles between the cables and **kt** in Fig. 2a) and the angle ε_L between **FL** and **kt** (ε_L is positive forward of **kt**). It can be assumed that the system flies with a fixed nominal separation angle selected in a tradeoff between increased safety (larger helicopter separation) and decreased penalty (smaller separation) as discussed below.

$$\tau 1 = \mathrm{FL}\frac{\sin(\xi 2 - \varepsilon_L)}{sin\sigma}$$
$$\tau 2 = \mathrm{FL}\frac{\sin(\xi 1 + \varepsilon_L)}{sin\sigma} \quad (2)$$

The load-sharing ratio is

$$\zeta = \frac{\tau 1}{\tau 2} = \frac{\sin(\xi 2 - \varepsilon_L)}{\sin(\xi 1 + \varepsilon_L)} \quad (3)$$

This ratio depends on ε_L and the key values are:

if $\varepsilon_L = \xi 2$: then $\varsigma = 0$ and cable 1 collapses (**FL** is aligned with cable 2)
if $\varepsilon_L = -\xi 1$: then $\varsigma = \infty$ and cable 2 collapses (**FL** is aligned with cable 1) (4)
if $\varepsilon_L = .5(\xi 2 - \xi 1)$: then $\varsigma = 1$ and cable tensions are equal

For equal cable lengths ($\xi 1 = \xi 2 = \sigma/2$) equal loading is obtained at $\varepsilon_L = 0$ and a cable collapses at $\varepsilon_L = \pm\sigma/2$. Thus, to fly the system with equal loading, the hook-to-hook line segment, **r21**, must be maintained perpendicular to the apparent load, **FL**. This is the basic rule for flying the system through a mission with equal loading in the case of equal cable lengths and for any formation angle. For unequal cable lengths, equal loading is obtained by maintaining **r21** offset from perpendicular to **FL** by a fixed angle $(\xi 2 - \xi 1)/2$.

If the load-sharing ratio, ς, is specified for, say, a UH-60 flying with a CH53 according to the ratio of their payloads, then the corresponding value of ε_L is given by inverting Eq. 3:

$$\tan\varepsilon_L = \frac{\sin\xi 2 - \varsigma \sin\xi 1}{\cos\xi 2 + \varsigma \cos\xi 1} \quad (5a)$$

For equal cable lengths this simplifies to

$$\tan\varepsilon_L = \frac{1 - \varsigma}{1 + \varsigma}\tan\sigma/2 \quad (5b)$$

A penalty function for the use of dual lift instead of a single helicopter can be defined as the excess cable tensions that must be carried by the helicopters:

$$P = \frac{\tau_1 + \tau_2}{FL} - 1 \quad (6a)$$

For equal loading this simplifies to

$$P = \frac{1}{\cos \sigma/2} - 1 \tag{6b}$$

A plot of this function for several load-sharing ratios is shown in Fig 3. The penalty is 5% of FL at 36 deg separation and about 15% at 60 deg for all load sharing ratios.

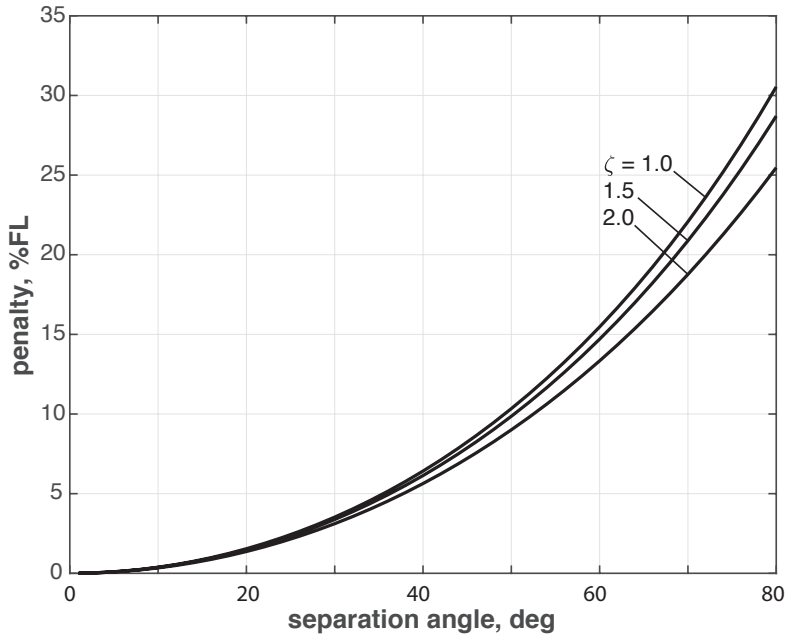

Figure 3. Pendant dual lift penalty vs separation angle (equal cable lengths)

Safety is related to the distance between helicopters in terms of rotor diameters and two diameters is tentatively considered a minimum. A given distance between helicopters can be achieved at lower separation angles (lower penalty) by using longer cables and shorter cables would require larger separation angles (larger penalty).

Sensitivity of cable tensions to variations in ε_L and σ are of interest. Formulas for these derivatives evaluated at equal loading are

$$\frac{\partial \tau 1}{\partial \sigma} = \frac{\partial \tau 2}{\partial \sigma} = FL^* \frac{\tan \sigma/2}{2 \cos \sigma/2}$$
$$\frac{\partial \tau 1}{\partial \varepsilon_L} = -\frac{\partial \tau 2}{\partial \varepsilon_L} = FL^* \frac{1}{2 \sin \sigma/2} \tag{7}$$

These are shown in Fig. 4 as a percent of FL per deg. Sensitivity to variations in cable separation angle are low and increase with σ to 0.25 %FL/deg at 60 deg separation. Sensitivity to misalignment with **FL** is larger (3%FL/deg at σ = 36 deg and 1.6%FL/deg at σ = 60 deg).

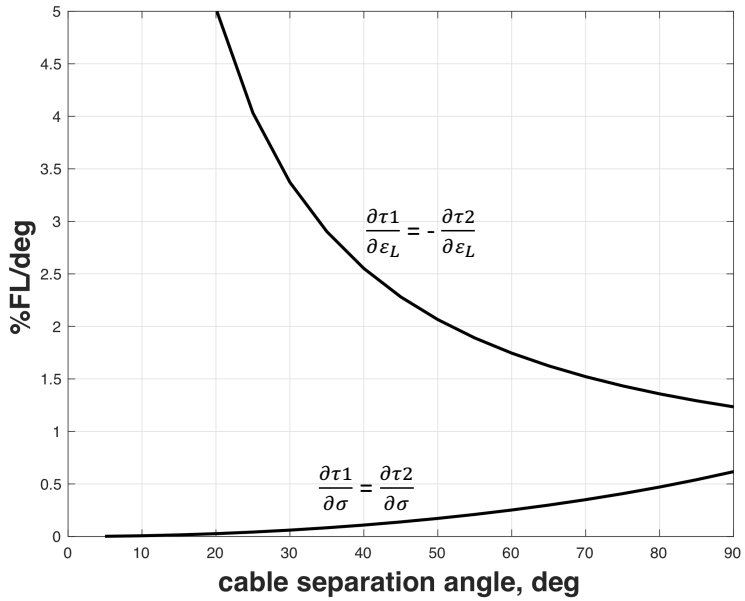

Figure 4. Cable tension sensitivity to variations in σ, ε_L (equal loading)

2.2 Apparent Load Identity. The force balance analysis above provides information valid for any formation of the helicopters (in line, side by side or in between). That is, cable tensions are independent of formation angle. The influence of formation angle (defined in Fig. 2(b)) can be obtained from the apparent load identity. Assuming that the elements of **FL** are known in level heading axes (local vertical axes with x in the direction of the flight path) then the direction of **FL** in triangle axes is related to the direction of **FL** in level heading axes by a transformation:

$$ul_T = T_{Th}(\phi_T, \theta_T, \psi_T)*ul_h \tag{8a}$$

Here, T_{Th} is the transformation from level heading axes to triangle axes given in terms of the Euler angles relating the two axes and **ul** is the unit direction vector of **FL**. Equation 2.8a can be expanded to

$$\begin{bmatrix} \sin\varepsilon_L \\ 0 \\ \cos\varepsilon_L \end{bmatrix} = E_1(\phi_T)*E_2(\theta_T)*E_3(\psi_T)\begin{bmatrix} ulx \\ uly \\ ulz \end{bmatrix} \tag{8b}$$

Here, the components of ul_h are ulx (representing speed rate and load drag) and uly (representing turn accelerations). In general, load weight and lift are distributed to all three path axes but predominantly to ulz. The angle θ_T, is the pitch of the hook-to-hook line segment, **r21,** and ϕ_T is the roll of the triangle plane about **r21** from the vertical plane defined by (**it, k)** (see Fig. 2(c)).

Equation 8(b) can be solved for triangle roll and pitch in terms of the remaining variables:

$$\begin{bmatrix} \sin\varepsilon_L \\ 0 \\ \cos\varepsilon_L \end{bmatrix} = E_1(\phi_T)*E_2(\theta_T)*E_3(\psi_T)\begin{bmatrix} ulx \\ uly \\ ulz \end{bmatrix} \tag{8b}$$

$$\begin{aligned} \sin\phi_T &= (\sin\psi_T * ulx - \cos\psi_T * uly) / \cos\varepsilon_L \\ \tan\Sigma &= (\cos\psi_T * ulx - \sin\psi_T * uly) / ulz \\ \sin(\theta_T - \Sigma) &= -\sin\varepsilon_L \cos\Sigma / ulz \end{aligned} \tag{9}$$

The angles on the left are less than 90 deg in this context. The result for θ_T is obtained from the x-equation in Eq. 8(b). The result for ϕ_T is obtained by multiplying the y-equation by cos ϕ_T and the z-equation by sin ϕ_T and subtracting the two. These results for triangle attitude are independent of the apparent load magnitude, and are valid for general formation angle and load sharing ratio (equivalent to ε_L).

Equations 2 and 9 suffice for an algorithm to solve the general configuration management problem that, in the case of equal cable lengths, can be stated as:

Given: FL_h, ψ_T, ς, σ
Find: $\tau 1$, $\tau 2$, ϕ_T, θ_T

The formation angle ψ_T is expected to be fixed throughout a mission, corresponding to an in-line or side-by-side formation or any intermediate angle. In flying a mission, the trail helicopter can control θ_T by controlling its height relative to the lead helicopter in accordance with the algorithm in order to maintain the prescribed load-sharing ratio, while ϕ_T, $\tau 1$, $\tau 2$ adjust automatically as required to satisfy the force balance equation.

The fixed formation angle can be selected, for example, to obtain the simplest requirements for configuration management activity during a mission. Formation angle can also be varied during a mission if useful. In principle, the roles of ψ_T and θ_T can be interchanged in the algorithm; that is, a fixed value of θ_T can be specified and ψ_T varied as required to maintain the specified load-sharing ratio, but this requires large rapid configuration rotations when transitioning from one segment of the mission to the next.

The remaining work in this report assumes equal cable lengths.

2.3 Sample Mission. A sample mission is shown in Fig. 5 within the flight envelope of the UH-60 and represents the trajectory of the lead helicopter cg. The trajectory was generated as a sequence of segments with steady speed (straight lines and turns) plus the accelerating segments connecting them (speed changes, turn entries and exits, pitch over and pull up). The connecting segments are defined with continuous acceleration and within limits on acceleration and acceleration rates appropriate to the UH-60 or further narrowed for dual lift operations. The method of imposing these limits is given in Appendix A. The major segments of the trajectory

are; (1) climb at 10 deg, 20 kts; (2) pitch over to level flight and accelerate to 100kts; (3) 180 deg turn; (4) pitch over to -10 deg and; (5) descend and decelerate to hover. Time histories of velocity (V, ψ, γ) and path axes accelerations ($\dot{v}$, $V\dot{\psi}cos\gamma, V\dot{\gamma}$) are given in Fig. 6.

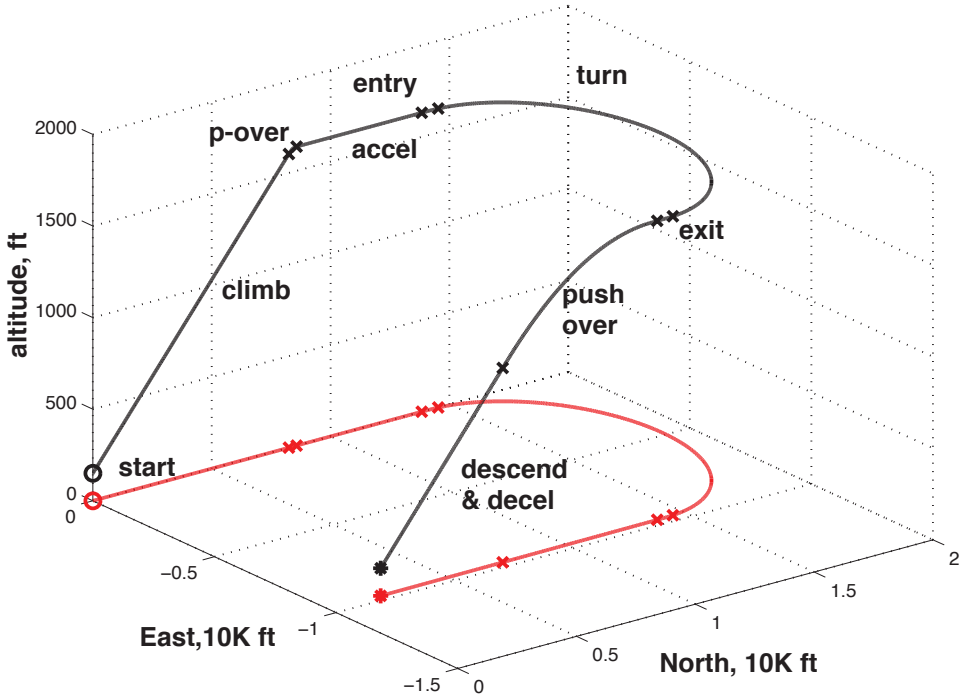

Figure 5. Sample mission profile

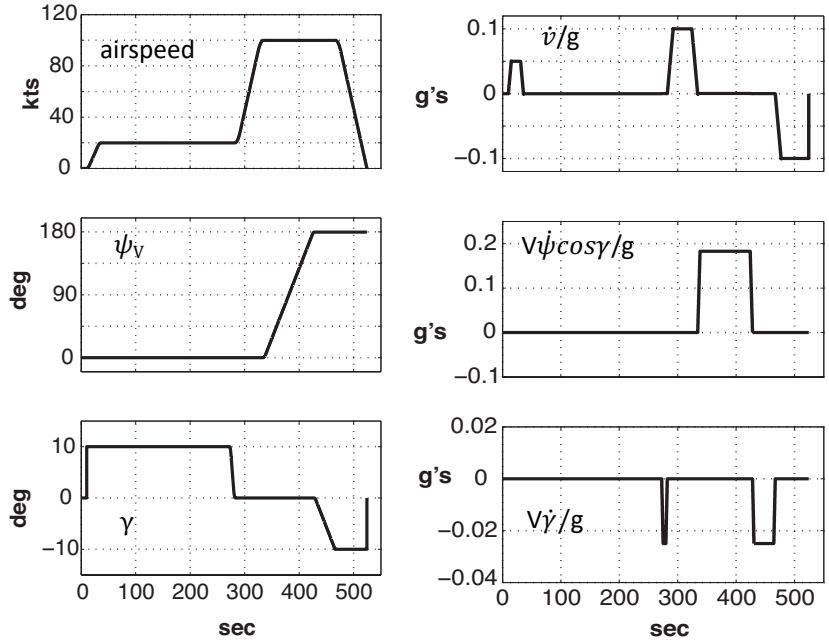

(a) velocity (b) acceleration

Figure 6. Reference trajectory velocity and acceleration

2.4 Configuration Variations during the Sample Mission. The triangle pitch and roll for equal cable tensions and various formation angles can be calculated using the configuration management algorithm defined above. The pendant geometry is an equilateral triangle with three UH-60 rotor diameters between hooks (162 ft) carrying a 9000 lb load with drag corresponding to an equivalent flat plate area of 120 ft^2. The drag relative to load weight is sufficient for **FL** to trail the vertical by more than 20 deg at 100kts. The results for these angles are independent of the scale of the system, whether small autonomous rotorcraft or full-scale helicopters carrying a load with the same drag to weight characteristics.

Triangle pitch and roll for equal load distribution are shown in Fig. 7 for formation angles of 0, 45, 90 deg. In these results, triangle pitch represents configuration control activity; that is, the trail helicopter vertical position relative to the lead helicopter would be varied as required to obtain the triangle pitch angle for equal loading. Triangle roll adjusts automatically to meet the requirements of force balance. For the inline formation (Fig. 7(a)), triangle pitch is active during accelerations and to balance load drag and triangle roll is active only to execute turns. Triangle pitch angles to about 25 deg nose down are required to balance load drag. For the side-by-side formation (Fig. 7(c)), the opposite occurs; that is, triangle pitch is active only during steady turns and otherwise the required triangle pitch angles are zero. Most of the activity is in triangle roll, which adjusts itself automatically to account for accelerations and load drag. For the 45 deg formation (Fig. 7b), triangle pitch is active during all maneuvering. These results indicate that the side-by-side formation requires configuration control activity only during turns and may be the simplest formation to manage. The corresponding altitude difference between the helicopters (h2 – h1) in the case of the example UH-60 system is shown in Fig. 8. The maximum height difference is 45 ft for the inline formation and 20 ft for the side by side. The periods when relative height is varied or held at a nonzero value are compared in the figure; the side-by-side formation requires the least such variations during the mission.

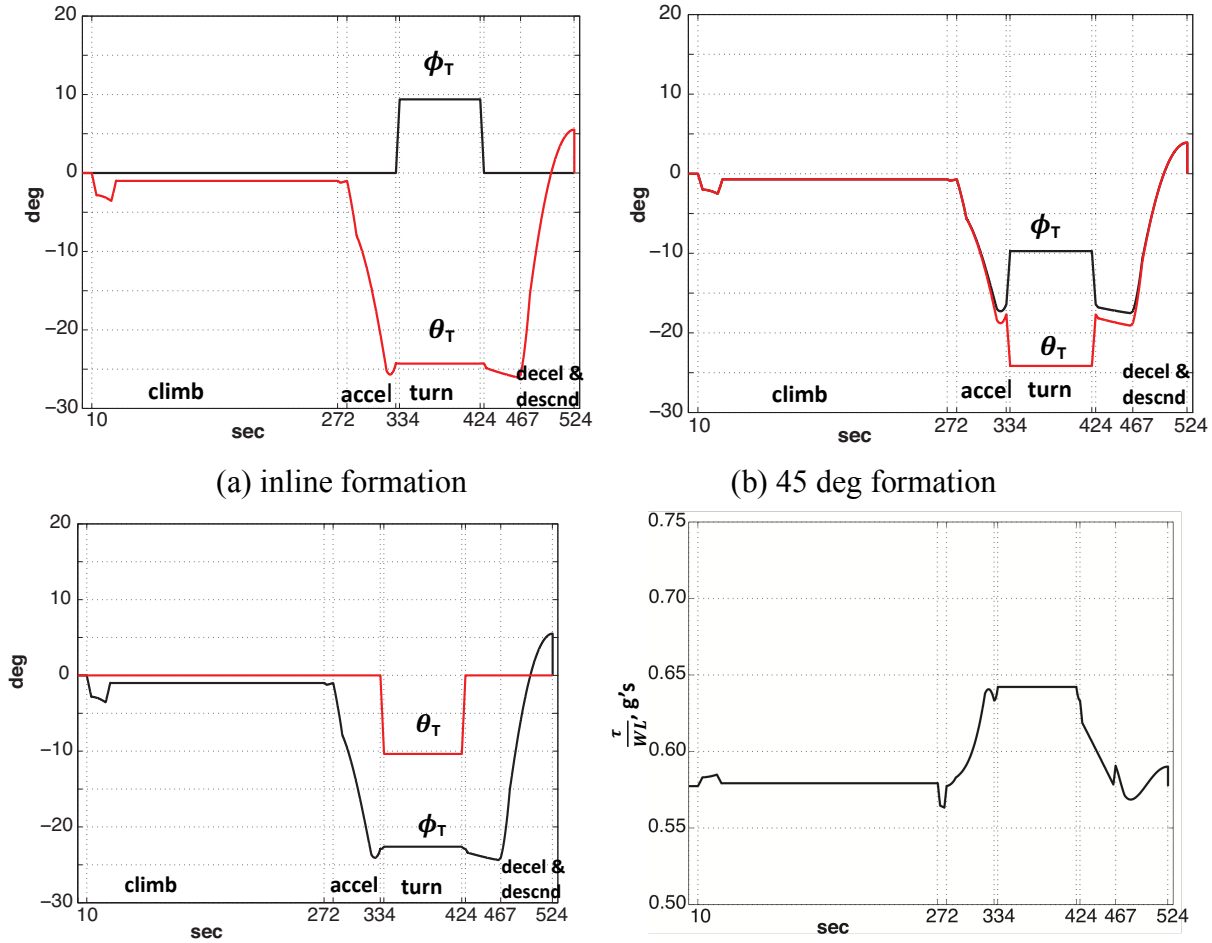

(a) inline formation

(b) 45 deg formation

(c) side by side formation

(d) cable tension, all formations

Figure 7. Configuration variations during a mission

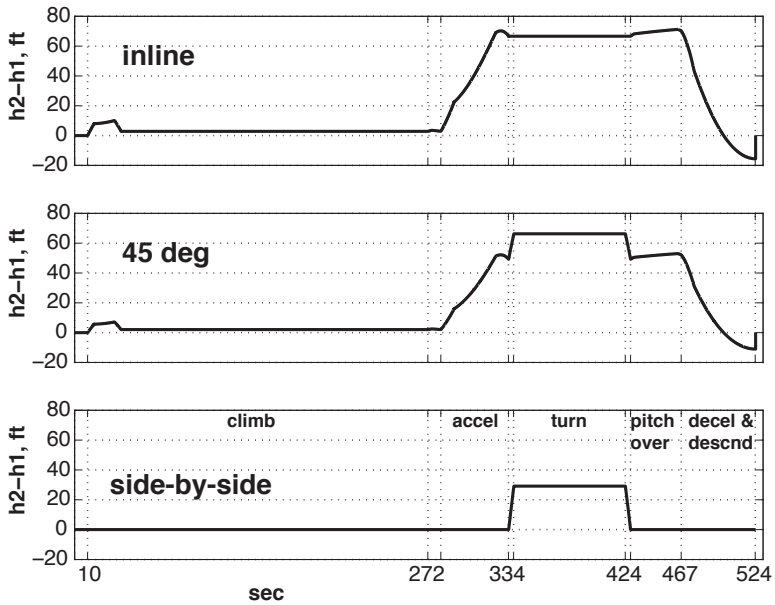

Figure 8. Relative height of the helicopters

Cable tensions are independent of formation angle and depend on **FL**, the load sharing ratio and the cable separation angle (Eq. 3). Results for the sample trajectory with equal loading are given in Fig. 7d as a fraction of the load weight. In hover cable tension is larger than 0.5WL due to the penalty of using dual lift, and otherwise increases moderately due to acceleration to 100 kts, load drag, and the steady turn. Load drag has the strongest effect here and also in the requirement for configuration adjustments to maintain equal loading seen in Figs. 7(a, b, c).

2.5 Sensitivities. In flight, the helicopters can vary ψ_T, θ_T and the separation distance L12 to regulate the system and there will be corresponding variations in the dependent variables $\tau 1$, $\tau 2$, ϕ_T, given by the derivatives

$$\frac{\partial(\tau 1, \tau 2, \phi_T)}{\partial(\psi_T, \theta_T, \mathrm{L12})}$$

The cable tension sensitivities are of interest in the control of cable tensions. The triangle roll sensitivities are of interest towards understanding which variations excite the pendulum. Analytical expressions can be derived from Eqs. 2 and 8(b) and are given in Appendix B.

Numerical results are given in Fig. 9 for the same configuration and load as in the sample mission. Calculations were made for static equilibrium flight (uly = 0, **FL = W + D**). Derivatives are given for the difference in cable tensions, $\Delta\tau = \tau 1 - \tau 2$, in the figure. A tension equalization controller would work on nulling this difference.

Formation angle variations (Fig. 9(a)) have no effect on $\Delta\tau$ for the inline configuration and otherwise depend on airspeed, reaching at most 1.3%FL per deg for the side-by-side formation at 100 kts. Thus, the coupling of formation angle to cable tensions is none to moderate depending on airspeed and formation. Triangle pitch (Fig 9(b)) has a larger effect at 3.5%FL per degree and, importantly for the design of a tension controller, this is very nearly invariant (as a % of FL) with formation angle and airspeed out to 100 kts. For equal loading there is no effect of hook separation, L12, on the difference in cable tensions (shown in appendix B); that is, variations in separation have an equal effect on each cable tension but the difference remains zero so that the tension difference can be controlled independent of separation control.

The derivatives of ϕ_T with hook separation and triangle pitch are both zero in this context. Only ψ_T excites triangle roll (Fig. 9(c)) and primarily for the inline formation at high speeds and at no more than 0.4 deg of roll per degree of formation angle variation for the range of the computations.

A configuration director or a feedforward control element to manage the configuration may depend on knowing the apparent load vector, FL_h, sufficiently accurately. Drag is the dominant load aerodynamic force in **FL** for most slung loads, and errors in estimating the drag are a source of errors in equalizing cable tensions by feed-forward control. The derivative of cable tension difference with load drag coefficient,

$$\frac{\partial(\Delta\tau)}{\partial \mathrm{CD}}$$

in Fig. 9(d) shows that there is no sensitivity for the side-by-side formation (load drag errors result only in errors in the predicted triangle roll and triangle roll is self-adjusting). Thus, for the side-by-side formation, the control of tension is unaffected by errors in estimating drag. For the inline formation sensitivities increase with airspeed (with drag) reaching 30%FL per unit CD at 100 kts. Thus, an error of 0.1 in estimating CD can result in a 3% FL difference in cable tensions at 100 kts for the in-line formation. Such errors can be corrected by feedback. In the absence of feedforward configuration management, the feedback alone would account for the gross effects of acceleration and load drag on load distribution as well as regulate the load distribution.

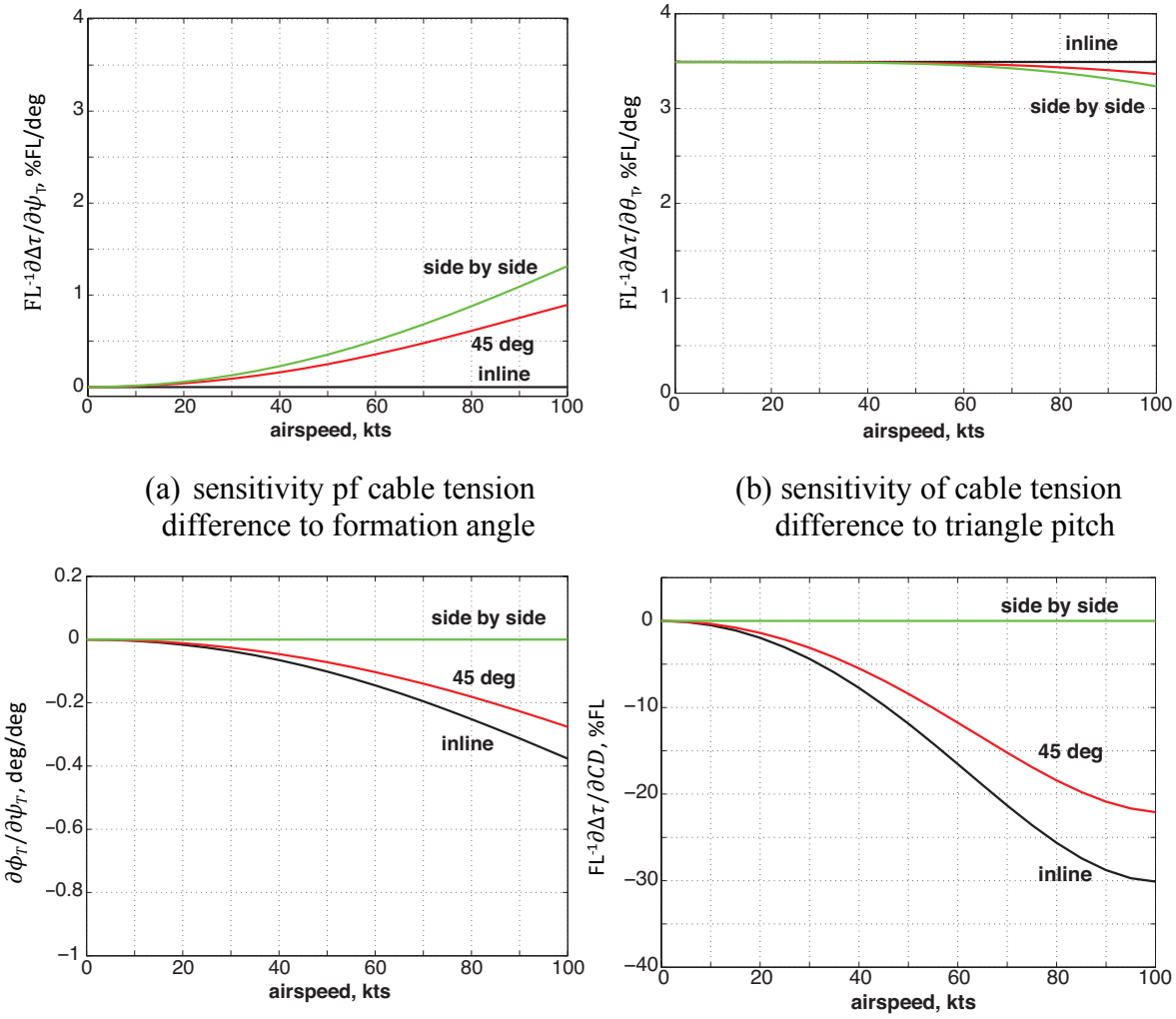

(a) sensitivity pf cable tension difference to formation angle

(b) sensitivity of cable tension difference to triangle pitch

(c) sensitivity of triangle roll to formation angle

(d) sensitivity of cable tension difference to CD

Figure 9. Sensitivities

The computations for Fig. 9 assumed static equilibrium, equal loading, 60 deg separation angle, and the load weight and drag characteristics of the previous analysis. Additional computations were made for (1) unequal loading ($\varsigma = 1.5$), (2) steady turns (0.5g lateral acceleration), (3) no drag and (4) 30 deg separation angle to determine if the characteristics noted above apply more

widely. Detailed results are given in Appendix B. In all cases the tension derivative with triangle pitch had the same or nearly the same invariance with airspeed and formation angle seen Fig 9(b), but varied in magnitude depending on separation angle.

2.6 Section Summary. This section analyzed the pendant suspension. The immediate question was how to fly the system to maintain the prescribed load sharing ratio while executing mission maneuvers. Results are derived from (1) force balance at the load attachment point and (2) the relation between the apparent load vector supported by the system as seen in level heading axes to the apparent load as seen in the plane of the pendant triangle. Key findings from the analysis are:

1. The apparent load was identified as the basic factor in managing the system configuration to maintain a prescribed load-sharing ratio. For equal loading of the two helicopters and equal cable lengths the general flight rule is to maintain the hook-to-hook line segment perpendicular to the apparent load. This rule can be adjusted to account for unequal loading or unequal cable lengths. The angle between the hook-to-hook line segment and the apparent load can be controlled by adjusting the height of one helicopter relative to the other.
2. Configuration management activity depends on the formation angle of the system. For the inline formation, adjustments are needed to account for acceleration and load drag; for the side by side formation adjustments are needed to carry out turns; for a 45 deg formation adjustments are needed to carry out all quasi-steady maneuvering. For the inline formation it is necessary to estimate load drag to determine the required relative height; for the side-by-side formation, configuration management is independent of load drag. For that formation, variations in the roll (swing) of the pendant suspension account for accelerations and drag and this is self-adjusting to satisfy the force balance equation.

Additional findings are:

1. The penalty for dual lift vs single lift increases with cable separation angle. Safety depends on the distance between helicopters measured in rotor diameters. For a given distance between the helicopters, smaller separation angles imply longer cables (lower penalty) and shorter cables imply larger separation angles (higher penalty). Thus cable lengths for dual lift can become very large compared to the lengths of suspensions used in single lift.
2. Cable tensions are sensitive to variations in the angle of the hook-to-hook line segment relative to the apparent load and relatively insensitive to separation angle variations.
3. Sensitivity of the cable tension difference to variations in formation angle, relative height of the helicopters, the distance between them, and errors in estimating drag show that it is (1) sensitive to relative height (triangle pitch) and this sensitivity is nearly invariant with speed at all formation angles, (2) relatively insensitive to formation angle, (3) insensitive to distance, and (4) sensitive to drag estimation errors for the in-line formation and insensitive for the side-by-side formation.

These results indicate (1) there are useful advantages of the side-by-side formation compared to the inline formation and (2) load distribution is readily controlled using relative helicopter height and is largely insensitive to other controllable variables.

3. HELICOPTER TRIM AND SIMULATION RESULTS

The objective of this section is to determine the thrust and attitude requirements of the helicopters in the dual lift configuration. For this study it is useful to develop a simplified helicopter trim algorithm based solely on HC force balance, including the hook force. In this context, the trajectory is known, the applied forces are known in level heading axes or body axes, the thrust vector is assumed to lie along the body vertical axis and the helicopter heading is assumed aligned with the direction of flight. In that case, the pitch and roll direction angles of the required thrust vector in level heading axes are also the inertial pitch and roll attitude angles of the helicopter.

3.1 Helicopter Trim Algorithm. The applied forces on the helicopter are shown in Figure 10. These consist of Thrust (**T**), airframe aerodynamics (**FA**), hook force (**Fhk**) and weight. Tail rotor thrust has been neglected in this model. The trim algorithm allows for steady or slowly varying accelerations (**a**).

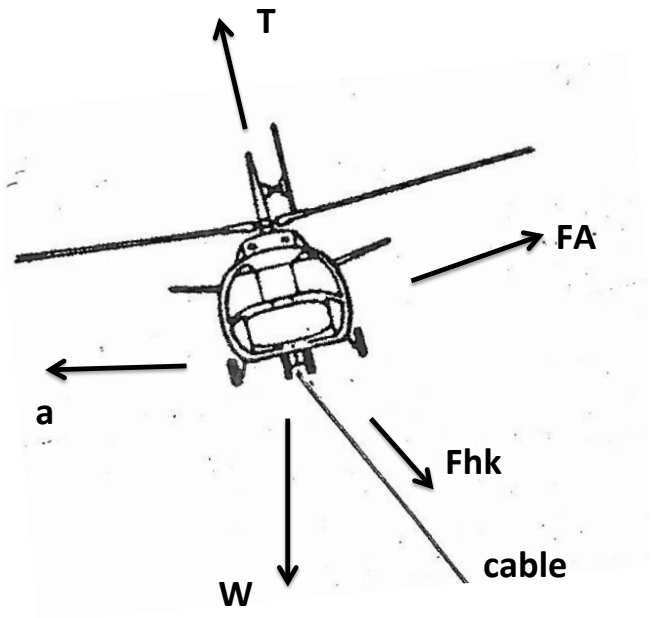

Figure 10. Forces applied to the helicopter

Force balance requires

$$\mathbf{T} = m\mathbf{a} - \mathbf{W} - \mathbf{Fhk} - \mathbf{FA} \tag{10a}$$

The vector equation can be expressed in level heading axes as

$$T_{hb}\, T_b = E_3\,(\psi_V)*m(a_N - g_N) - T_{hb}FA_b - Fhk_h \tag{10b}$$

Where T_{hb} is the transformation from body axes to level heading axes

$$T_{hb} = E_2(-\theta) * E_1(-\phi) \tag{11}$$

On the righthand side of Eq. 10b, the trajectory acceleration and velocity are known in inertial axes, the helicopter airframe aerodynamics, **FA**, will be given by body axes components tabulated as functions of angle of attack (α) and airspeed. Here, α is a dependent variable given from helicopter attitude and flight path angle by

$$\alpha = \tan^{-1}(\cos\phi * \tan(\theta - \gamma)) \tag{12}$$

The hook force vector can be given in level heading axes by trimming the pendant triangle as outlined in the previous section.

On the left-hand side of Eq. 10b the thrust vector, **T**, is assumed to lie along the body vertical axis. This is related to pitch and roll angles by transforming it to level heading axes

$$T_h = T * E_2(-\theta) * E_1(-\phi) * \begin{bmatrix} 0 \\ 0 \\ 1 \end{bmatrix} = T * \begin{bmatrix} \cos\phi * \sin\theta \\ -\sin\phi \\ \cos\phi * \cos\theta \end{bmatrix} \tag{13}$$

In this context, Eq 10b contains three unknowns, ϕ, θ, T, which, in view of Eq 13, can be given in terms of the right-hand side of Eq. 10b (rhs_h) as:

$$\begin{aligned} T &= |rhs_h| \\ \phi &= \sin^{-1}(rhs_h(2)/T) \\ \theta &= \tan^{-1}(rhs_h(1)/ rhs_h(3)) \end{aligned} \tag{14}$$

In Eq. 14 it is assumed that $|\phi|, |\theta| < 90$deg. Since ϕ, θ appear on both the left and righthand sides of Eq. 10b, then an iterative solution is required. These angles appear on the righthand side only in the airframe aerodynamics so that if the airframe aerodynamics can be neglected then the righthand side of Eq 10b is known and Eq. 14 is a closed form solution, but this is not the case in general.

3.2 Hook Force. The pendant trim algorithm of the previous section solves for $\tau 1$, $\tau 2$, ϕ_T, θ_T given FL_h, ψ_T, ς, σ. The cable directions between points 1 and 3 and between points 2 and 3 in Fig. 2 in triangle axes are:

$$k13_T = [-\sin\xi 1, 0, \cos\xi 1]^T$$
$$k23_T = [\sin\xi 2, 0, \cos\xi 2]^T$$

where $\xi 1$, $\xi 2$ are known from the geometry of the pendant.

Then the hook forces on helicopters 1 and 2 in level heading axes are

$$\begin{aligned} Fhk1_h &= \tau 1 * T_{hT} * k13_T \\ Fhk2_h &= \tau 2 * T_{hT} * k23_T \end{aligned} \tag{15}$$

where

$$T_{hT} = E_1(-\psi_T) * E_2(-\theta_T) * E_3(-\phi_T)$$

3.3 Helicopter Airframe Aerodynamics. These can be neglected for hover and low speeds but become significant in forward flight. Trims were obtained from the GenHel components and blade element model of the UH-60A developed at Sikorsky [20] and [21] and at Ames Research Center [22] beginning from the Sikorsky model of the 1980's. It has been validated statically and dynamically at Ames for use in pilot opinion studies. A GenHel-based utility that allows the user to specify the hook force vector was used for the calculations. Trims were generated for level flight at speeds from 0 to 120 kts in 10 kt increments with hook force direction in the X-Z plane varied to get trim angle of attack in the range of -20 to 20 deg at each airspeed. Sideslip angle is small or zero for the helicopter in trimmed quasi-steady maneuvering so that it is unnecessary to account for nonzero sideslip angles. These data were interpolated to common grids to get a table of the airframe aerodynamics as a function of angle of attack and airspeed and this is given in Appendix C. The data accounts for fuselage and empennage aerodynamics including main rotor downwash effects. Results are given in lbs of force and correspond to sea level standard day atmospheric conditions. These can be scaled by dynamic pressure to general atmospheric conditions and altitudes.

Figure 11 shows the airframe aerodynamics in both body and wind axes. At 100kts airframe drag reaches 1000 to 2000 lbs and lift reaches -4000 to 2000 lbs over the aoa range of the plot (±20 deg).

Airframe drag and lift vs aoa are shown in Fig 12.

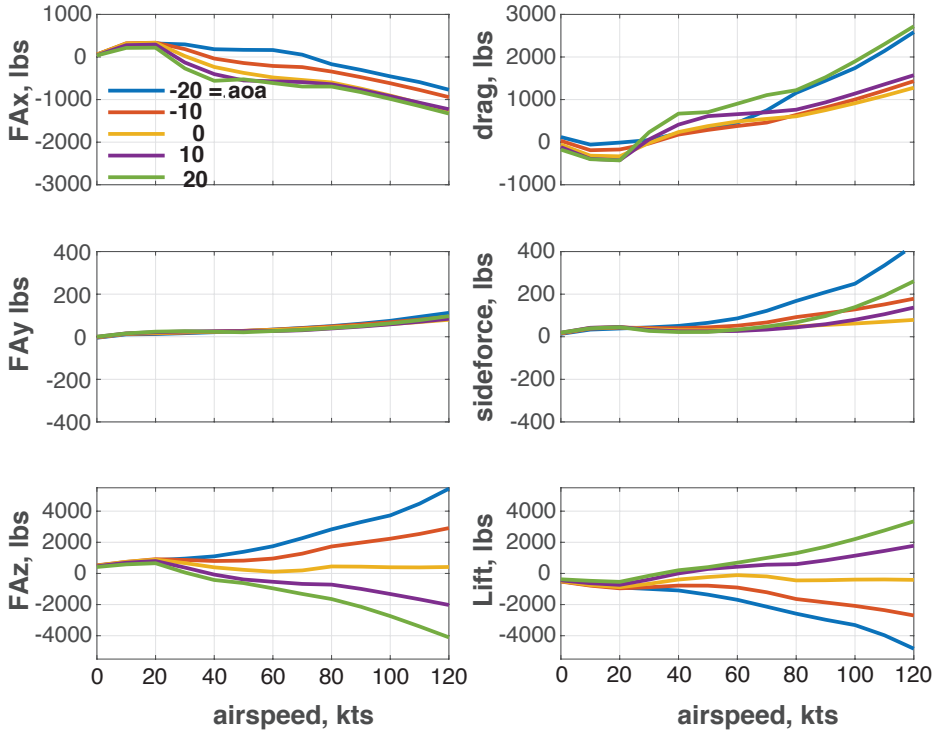

(a) body axes (b) wind axes

Figure 11. UH-60 airframe aerodynamics vs airspeed

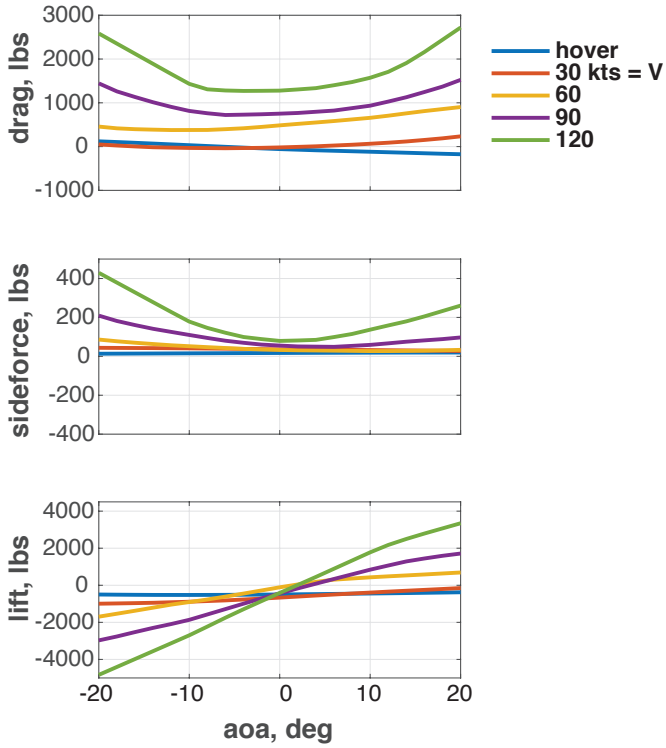

Figure 12. UH-60 Airframe aerodynamics vs aoa

3.4 Results along a Sample Mission. Helicopter trim results were obtained for the sample mission in Figs. 5 and 6 and the sample configuration of section 2 (UH-60 helicopters, equal loading, equal cable lengths, three rotor diameter helicopter separation, 60 deg cable separation angle, 9000 lb high drag load). Computations were made for formation angles in {0, 45, 90} deg. Helicopter weight was 14800 lbs, corresponding to the UH-60 with half fuel. The load and helicopter weights are sized to avoid exceeding the UH-60 thrust limit, which is taken to correspond to the 22000 lbs gross takeoff weight limit for the combined aircraft and payload. To recall, the trajectory consisted of a 10 deg climb at 20 kts, pitch over and level acceleration to 100 kts, 180 right turn, pitch over and a decelerating 10deg descent to hover. Matters of interest are thrust requirements and helicopter attitude angles as they vary with formation angle and between the lead and trail HC's.

Figure 13 shows the helicopter thrust and attitude requirements. During the low speed climb, the thrust requirements (Fig 13(a)) are the same for both helicopters and all formation angles because the apparent load on the system is at/near the vertical, the aerodynamics are negligible and the system rises with the helicopters level with each other regardless of formation angle. At 100 kts, thrust requirements differ between lead and trail HC's for the inline formation and are the same for the side-by-side formation. For the inline formation, differences in HC trim pitch attitude between lead and trail HCs result in significant differences in fuselage lift and, therefore, the required thrust. Figure 14 shows sketches of these configurations at 100 kts. If load drag is negligible then the thrust requirements in forward flight are about the same as for the 20 kt climb except for airframe aerodynamics and there would be little difference in thrust requirements with formation angle.

Helicopter attitude is shown in Figs. 13(b, c). Pitch has the same time history signature for all cases except to shift up or down depending on formation angle and lead or trail HC. The extreme pitch (-15 to -20 deg) occurs for the lead HC in the in-line formation and is principally due to load drag. Otherwise pitch is between10 deg down and 10 deg up. For the side-by-side formation, the pitch angle history is identical for the two helicopters and similar to that of a single helicopter carrying a slung load. Roll is identical for the two helicopters in the inline formation and similar to that of a single helicopter carrying out the mission maneuvers. For the side by side formation the helicopters are rolled 8-10 deg left and right from the roll of a single helicopter.

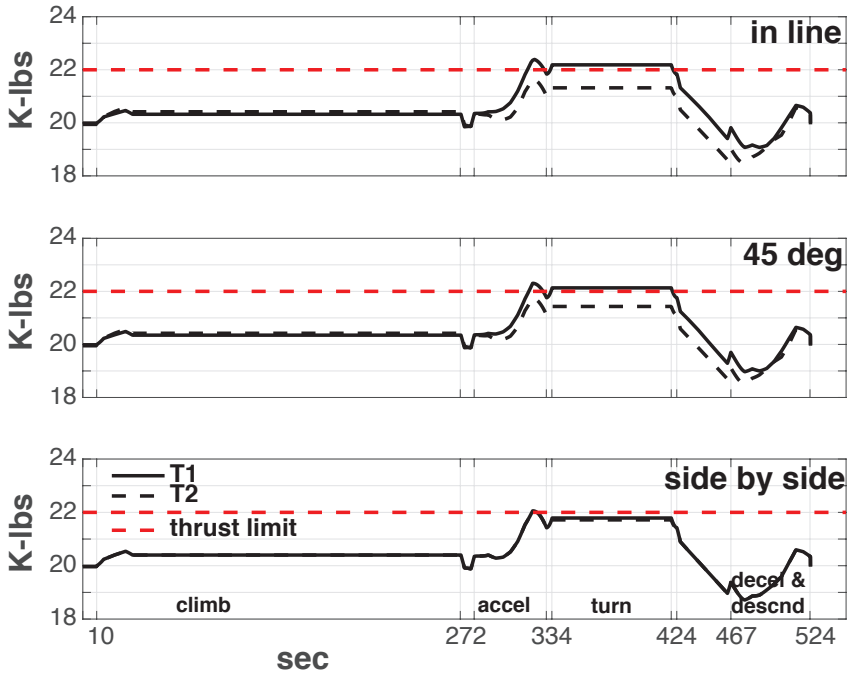

(a) thrust requirements

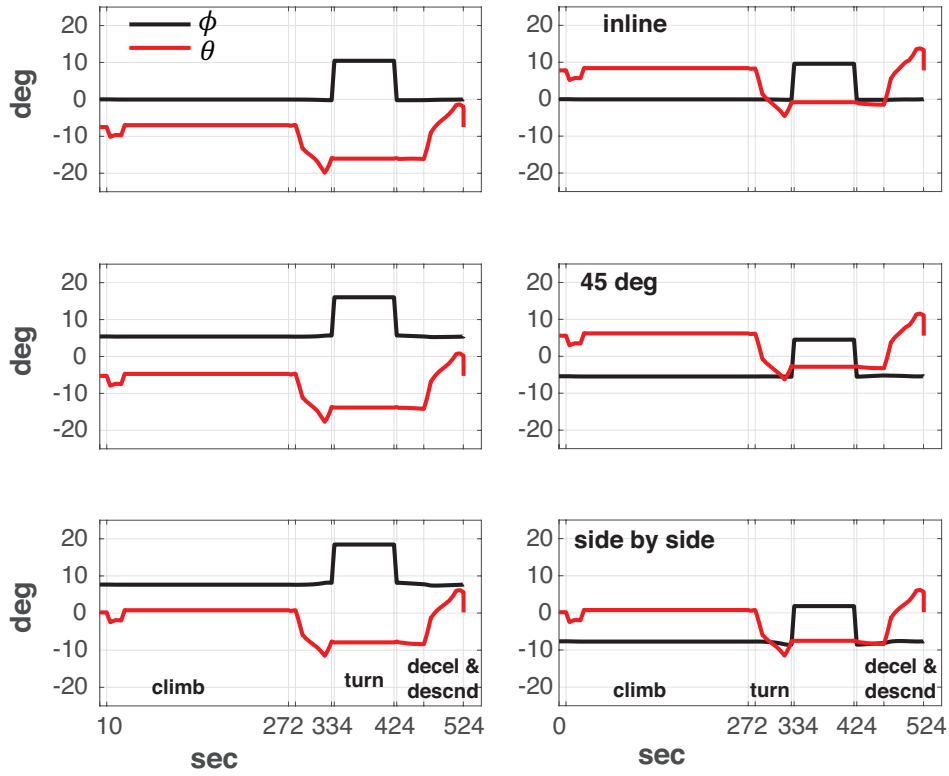

(a) lead HC attitude (b) trail HC attitude

Figure 13. Helicopter trim thrust and attitude along sample mission

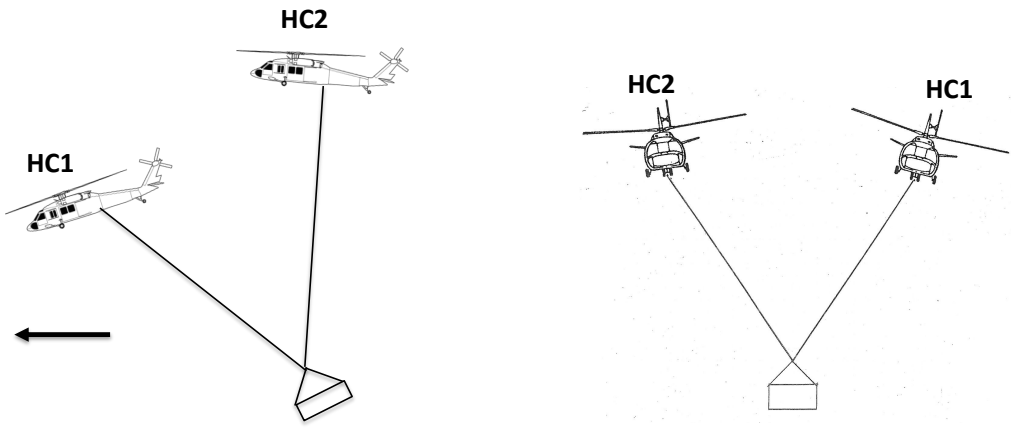

(a) inline formation (b) side by side formation

Figure 14. System Configurations at 100kts

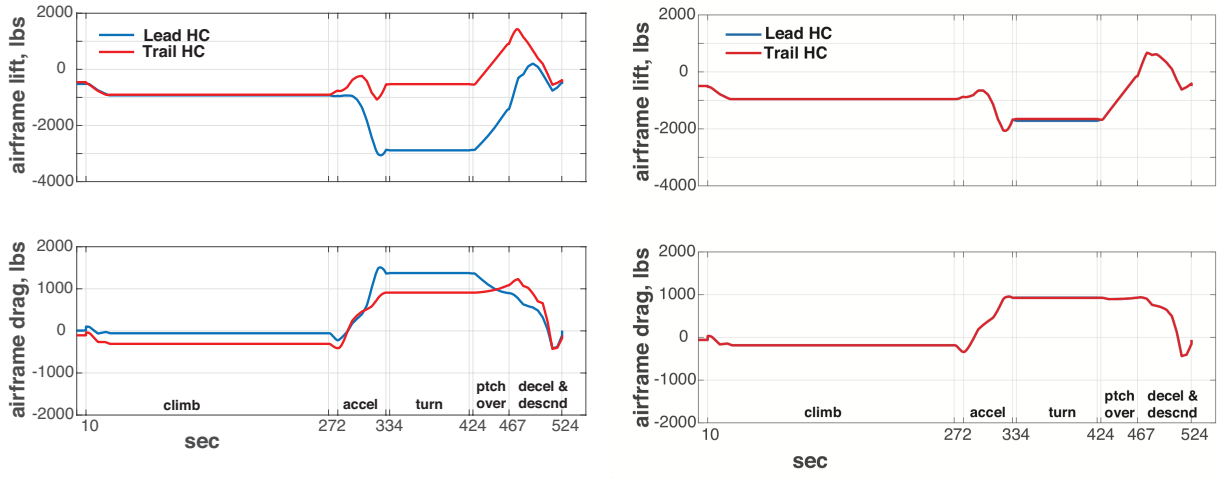

(a) inline formation (b) side by side formation

Figure 15. Airframe forces along sample mission

Figure 16 shows the cable angles relative to HC body axes. These are of interest to determine the proximity of the cables to the helicopters and whether there is a safety concern as a result of the pendant geometry combined with HC attitude. For single lift a safety limit of -45 deg relative pitch is usually imposed and this limit is appropriate for the in-line formation. Relative pitch for the lead HC in this case reaches -40 deg and is close to the limit. This results from load drag combined with the geometry of the pendant suspension and the formation angle. Otherwise there is no concern about forward cable pitch for the trail HC or risk due to the relative cable angles at other formation angles.

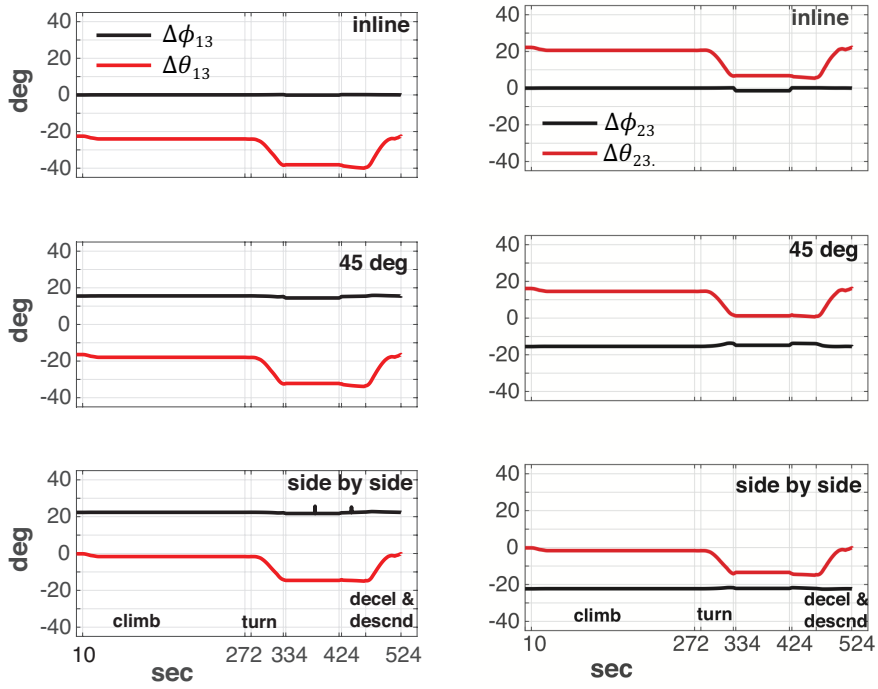

(a) lead HC (b) trail HC

Figure 16. Relative cable angles along sample mission

3.5 Section Summary. Requirements on helicopter thrust and attitude are examined in this section for an example UH-60 system with equal loading, equal cable lengths and three rotor diameters helicopter separation flying through the sample mission defined in Fig. 5. The general approach is based on force balance analysis of the helicopter trim in which the applied forces are balanced by a thrust vector along the vertical body axis and aircraft pitch and roll attitude are defined by the direction of the vertical body axis and the direction of flight. The analysis requires the airframe aerodynamics in trimmed flight and these have been tabulated in terms of aoa and airspeed from a GenHel simulation of the UH-60. Some results are:

- Thrust requirements for the two helicopters are identical for the side-by-side formation but not for the inline formation owing to large differences in helicopter pitch angle between lead and trail helicopter and this is due mostly to load drag. For this case the cable tensions are equal but the thrust requirements are not.
- Large negative helicopter pitch (-15 to -20 deg) is required for the lead helicopter in the inline formation due to load drag. Pitch history is identical for both HC's in the side-by-side formation.
- Roll angle is the same for both helicopters for the inline formation and consistent with that of a single HC carrying out the mission maneuvers. For the side by side formation the helicopters are tilted in roll left and right from that of a single helicopter carrying out the mission, and the tilt is close to 10 deg.
- Relative trail angles approaching the safety limit occur for the lead helicopter in the inline formation but are not otherwise a safety factor.

4. CONCLUSIONS

1. The apparent load to be supported by the helicopters at any time is the sum of load weight, aerodynamics and acceleration reaction. If the cable lengths are equal then the basic rule for maneuvering the system with equal loading of the two HC's is to maintain the hook-to-hook line segment perpendicular to the apparent load. This rule is independent of formation angle. For unequal cable lengths or prescribed unequal loading then a similar rule can be given for the orientation of the hook-to-hook line segment.

2. The relative height of the two helicopters must be varied during maneuvering in accordance with the rule and depending on formation angle. Results for equal cable lengths and equal loading along a reference mission trajectory that encompasses the typical repertoire of maneuvers show that:

- The inline formation requires relative height adjustments for accelerations and to balance load drag.
- The side by side formation requires relative height adjustments only during turns
- The 45 deg formation requires relative height adjustments during all maneuvering and to balance load drag.

3. The derivatives of cable tension difference with respect to the controllable configuration variables show that

- Cable tension difference is most sensitive to triangle pitch (relative helicopter height) and the sensitivity is invariant with airspeed and formation angle as a fraction of the apparent load.
- Cable tension difference is moderately coupled to formation angle, depending on airspeed and formation angle.
- Cable tension difference is decoupled from separation distance.
- In the side by side formation, load drag is balanced by triangle roll without any change in triangle pitch and without any effect on cable tension difference.

4. A simplified helicopter trim algorithm based on force balance was used to calculate the helicopter thrust and attitude requirements. Results along a typical mission using Black Hawk helicopters and estimated fuselage aerodynamics show that

- For the inline formation at high speeds, the thrust requirements differ between lead and trail helicopter due to differences in pitch attitude required by the direction of the hook forces and the corresponding differences in HC aerodynamic forces at high speed. In this case, equal cable tensions do not imply equal HC thrust magnitude.

- For the side by side formation, pitch and thrust requirements are identical for the two HC's at all times, while equal and opposite steady state roll angle is required relative to the roll of a single helicopter carrying out the same maneuvers, nearly 10deg in the example.

APPENDIX A. REFERENCE TRAJECTORY GENERATION

For the sample mission, a reference trajectory was constructed as a sequence of segments with steady speed (straight lines and turns) plus the accelerating segments connecting them (speed change, turn entry and exit, pitch over and pull up). The connecting segments are constructed with continuous acceleration and within the limits on acceleration and acceleration rate of the UH-60 and further reduced for dual lift maneuvering.

Limits are applied to the path axes components of acceleration. These separate the acceleration vector into components associated with changes in speed, heading, and flight path angle, respectively. Path axes are the tangent to the path (denoted **ip**), the right-wing lateral to the path in the horizontal plane (**jp**) and the downward perpendicular to the path in the vertical plane **(kp**).

Inertial velocity can be given in terms of V, ψ_V, γ as

$$V_N = V\begin{bmatrix} \cos\gamma\cos\psi_V \\ \cos\gamma\sin\psi_V \\ -\sin\gamma \end{bmatrix} \tag{16}$$

and then the inertial acceleration can be written in terms of path axes components as

$$\frac{dV_N}{dt} = \dot{V}\begin{bmatrix} \cos\gamma\cos\psi_V \\ \cos\gamma\sin\psi_V \\ -\sin\gamma \end{bmatrix} + V\dot{\psi}_V\cos\gamma\begin{bmatrix} -\sin\psi_V \\ \cos\psi_V \\ 0 \end{bmatrix} - V\dot{\gamma}\begin{bmatrix} \sin\gamma\cos\psi_V \\ \sin\gamma\sin\psi_V \\ \cos\gamma \end{bmatrix} \tag{17}$$

or

$$\frac{dV_N}{dt} = \dot{V}\, ip_N + V\dot{\psi}_V\cos\gamma\, jp_N - V\dot{\gamma}\, kp_N \tag{18}$$

or

$$\frac{dV_N}{dt} = E2(\gamma)*E3(\psi_V)\begin{bmatrix} \dot{V} \\ V\dot{\psi}_V\cos\gamma \\ -V\dot{\gamma} \end{bmatrix} \tag{19}$$

Once the path axes accelerations are defined then Eq. 19 can be used to transform to inertial axes for integration.

For continuous acceleration, a fixed small value of acceleration rate (jerk) is imposed. The acceleration rates and the limits on acceleration chosen for dual lift trajectory generation are given in Table 1.

Table 1. Kinematic limits on maneuvering

$\ddot{V}$	0.01 g/sec	$\ddot{\psi}$	0.5 deg/sec^2	$(\dot{V\gamma})$	0.01 g/sec
$\dot{V}$	0.05 g	$\dot{\psi}$	2 deg/sec	$V\dot{\gamma}$	0.025 g

For example, to define a change in steady state speed from V1 to V2 > V1 the steps are

1. Ramp up the speed rate, $\dot{V}$, at $\ddot{V}$= 0.01 g/sec from zero to max($\dot{V}$) = 0.05 G.
2. Hold max($\dot{V}$) until V reaches V2 less the amount of speed increase from step 1.
3. Ramp down $\dot{V}$, at $\ddot{V}$ = -0.01 g/sec to 0 (reverse step 1)

Speed reaches V2 at the same time that $\dot{V}$ = 0. Figure 17 illustrates these steps for a speed change from hover to 20kts. For speed decreases, signs are reversed. Note that jerk is a step function that jumps between zero and its limit values. This simplifies the code with little cost in terms of a trajectory that the physical system can track (discontinuous jerk corresponds to discontinuous control rate). The 3-step procedure fails if the change in speed is less than twice the speed change in step 1, but this minimum change is very small for the parameter values in table 1 and posed no actual problem.

Changes in heading and flight path angle are treated similarly. For the lateral axis, heading rate and its derivative are held within specified limits rather than lateral acceleration. This prevents the code from requiring large heading rates at low airspeeds.

Accelerations and acceleration rates on the reference trajectory map to control positions and control rates on the aircraft. For the present procedure the reference trajectory maps to continuous control positions but discontinuous control rates, which cannot be reproduced by the physical system. The result would be an error in tracking the commanded trajectory that then excites the trajectory tracking feedback. This error is expected to be negligible and momentary for the maneuver domain of a dual lift system.

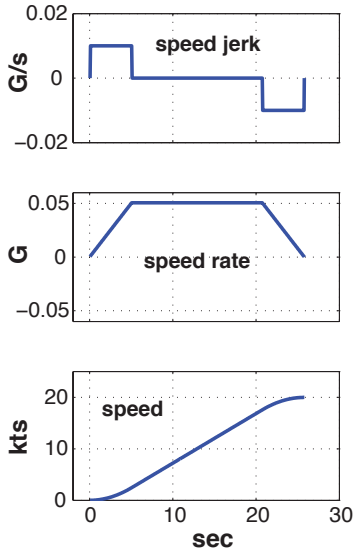

Figure 17. Example reference trajectory element: Speed change with rate and jerk limiting

APPENDIX B. SENSITIVITIES

This appendix provides formulas for the sensitivities of interest discussed in section 2; that is, the derivatives

$$\frac{\partial(\tau 1,\tau 2,\phi_T)}{\partial(\psi_T,\theta_T,\mathrm{L12})} \quad \text{and} \quad \frac{\partial(\tau 1,\tau 2)}{\partial \mathrm{CD}}$$

The formulas were derived from Eqs. 2 and 8b of the text, which are repeated here:

$$\tau 1 = \mathrm{FL}\frac{\sin(\xi 2 - \varepsilon_L)}{sin\sigma}$$
$$\tau 2 = \mathrm{FL}\frac{\sin(\xi 1 + \varepsilon_L)}{sin\sigma} \tag{2}$$

$$\begin{bmatrix} \sin\varepsilon_L \\ 0 \\ \cos\varepsilon_L \end{bmatrix} = \mathrm{E_1}(\phi_\mathrm{T})*\mathrm{E_2}(\theta_T)*\mathrm{E_3}(\psi_T)\begin{bmatrix} \mathrm{ulx} \\ \mathrm{uly} \\ \mathrm{ulz} \end{bmatrix} \tag{8b}$$

Analytical expressions for the derivatives of cable tensions are given in Fig. 18 and those for triangle roll in Fig. 19. The expressions are for equal cable length. A review of their derivation is omitted.

Sensitivities of the cable tension difference to the top-level controllable variables of the pendant dual lift configuration are of interest in controlling the load distribution to the two helicopters. Numerical results for equal loading and static equilibrium were given in Fig. 9 of the text and discussed there. For this case the results showed that

1. Cable tension difference was sensitive to triangle pitch and the sensitivity was nearly invariant with airspeed and formation angle.
2. Coupling between tension difference and formation angle variations was zero to moderate depending on airspeed and formation angle. There is no coupling for the side-by-side formation.
3. There is no sensitivity of tension difference to helicopter separation.

The object of this appendix is to determine if these characteristics extend more generally to unequal loading and accelerating flight.

Effects of unequal loading and steady turns on the sensitivities. Figure 20 compares derivatives for (1) the reference case (equal cable lengths, equal loading, static equilibrium), (2) the same except unequal loading with loading ratio 1.5, and (3) the same except a steady turn with lateral acceleration = 0.5g.

Figure 20(a) shows the derivative of the difference in tension with formation angle. In the reference case, the derivatives are 0 to 1.3% FL per degree, depending on speed and formation angle and the side-by-side formation has no sensitivity to formation angle at any speed. These derivatives are unaffected by unequal loading. However, there is increased coupling during turns. For the inline formation this occurs at all airspeeds and for the side-by-side formation it increases with airspeed and is in the range of 0 to 1%FL/deg.

Figure 20(b) shows the tension derivatives with triangle pitch. These are essentially invariant with airspeed and formation angle and have the same magnitude (approximately 3 to 3.4%FL/deg) independent of load sharing and turn acceleration.

Figure 20(c) shows the derivative of cable tension difference with helicopter separation, L12. Units are %FL per % L12. This is independent of formation angle and is zero for equal loading, whether straight line or turning flight so that separation and tension control are decoupled. The cable tensions vary with L12 but in equal amounts so that the difference remains zero. For unequal loading there is nonzero coupling. For the example case ($\zeta = 1.5$) this is 0.23%FL per %L12 independent of airspeed and formation angle. For the UH-60 system considered here, 1% L12 is 1.6 ft.

Figure 20(d) shows the cable tension derivatives with CD. For the side-by-side formation, cable tension differences are insensitive or nearly insensitive to errors in estimating CD at all airspeeds, but not for the other formations. Sensitivities are large in the figure because they are given per unit CD. For a CD estimation error of .1, the corresponding values would be one tenth of the value shown, of size 3% FL at 100 kts for the inline formation.

Summary. The conclusions given for cable tension difference in the case of equal loading in static equilibrium flight apply also to unequal loading and lateral acceleration in turns except that lateral acceleration introduces some coupling with formation angle variations and that unequal loading introduces minor coupling with separation distance. Triangle pitch is the principal means of controlling cable tension difference and its sensitivity to pitch is nearly invariant with airspeed, formation angle, loading ratio, and acceleration.

$$\frac{\partial \tau 1}{\partial \psi_T} = \frac{\partial \tau 1}{\partial \varepsilon_L}\frac{\partial \varepsilon_L}{\partial \psi_T} \qquad \frac{\partial \tau 2}{\partial \psi_T} = \frac{\partial \tau 2}{\partial \varepsilon_L}\frac{\partial \varepsilon_L}{\partial \psi_T}$$

$$\frac{\partial \tau 1}{\partial \theta_T} = \frac{\partial \tau 1}{\partial \varepsilon_L}\frac{\partial \varepsilon_L}{\partial \theta_T} \qquad \frac{\partial \tau 2}{\partial \theta_T} = \frac{\partial \tau 2}{\partial \varepsilon_L}\frac{\partial \varepsilon_L}{\partial \theta_T}$$

$$\frac{\partial \tau 1}{\partial \mathrm{L12}} = \frac{\partial \tau 1}{\partial \sigma}\frac{\partial \sigma}{\partial \mathrm{L12}} \qquad \frac{\partial \tau 2}{\partial \mathrm{L12}} = \frac{\partial \tau 2}{\partial \sigma}\frac{\partial \sigma}{\partial \mathrm{L12}}$$

$$\frac{\partial \tau 1}{\partial \mathrm{CD}} = -\frac{\mathrm{Q\ S_{ref}}}{\sin\sigma}\left(\sin(.5\sigma - \varepsilon_L)\ \mathrm{ulx} + \cos(.5\sigma - \varepsilon_L)\mathrm{FL}\frac{\partial \varepsilon_L}{\partial \mathrm{D}}\right)$$

$$\frac{\partial \tau 2}{\partial \mathrm{CD}} = -\frac{\mathrm{Q\ S_{ref}}}{\sin\sigma}\left(\sin(.5\sigma + \varepsilon_L)\ \mathrm{ulx} - cos(.5\sigma + \varepsilon_L)\mathrm{FL}\frac{\partial \varepsilon_L}{\partial \mathrm{D}}\right)$$

where

$$\frac{\partial \varepsilon_L}{\partial \psi_T} = \frac{\cos\theta_T\left(-\sin\psi_T \mathrm{ulx} + \cos\psi_T \mathrm{uly}\right)}{\cos\varepsilon_L}$$

$$\frac{\partial \varepsilon_L}{\partial \theta_T} = -\frac{\sin\theta_T\left(\cos\psi_T \mathrm{ulx} + \sin\psi_T \mathrm{uly}\right) + \cos\theta_T \mathrm{ulz}}{\cos\varepsilon_L}$$

$$\frac{\partial \tau 1}{\partial \varepsilon_L} = -\mathrm{FL}\frac{\cos\left(.5\sigma - \varepsilon_L\right)}{\sin\sigma}$$

$$\frac{\partial \tau 2}{\partial \varepsilon_L} = \mathrm{FL}\frac{\cos\left(.5\sigma + \varepsilon_L\right)}{\sin\sigma}$$

$$\frac{\partial \tau 1}{\partial \sigma} = \mathrm{FL}\frac{\cos\left(.5\sigma - \varepsilon_L\right)}{\sin\sigma}\left(\frac{1}{2} - \frac{\tan\left(.5\sigma - \varepsilon_L\right)}{\tan\sigma}\right)$$

$$\frac{\partial \tau 2}{\partial \sigma} = \mathrm{FL}\frac{\cos\left(.5\sigma + \varepsilon_L\right)}{\sin\sigma}\left(\frac{1}{2} - \frac{\tan\left(.5\sigma + \varepsilon_L\right)}{\tan\sigma}\right)$$

$$\frac{\partial \sigma}{\partial \mathrm{L12}} = \frac{2}{\mathrm{L12}}\tan\sigma$$

$$\mathrm{FL}\frac{\partial \varepsilon_L}{\partial \mathrm{D}} = \left(-\sin\theta_T \mathrm{ulx} + \cos\psi_T \cos\theta_T \mathrm{ulz}\right)\frac{\mathrm{ulz}}{\cos\varepsilon_L}$$

Figure 18. Derivatives of cable tensions

$$\frac{\partial \phi_T}{\partial \psi_T} = \left(\frac{\cos\psi_T \mathrm{ulx} + \sin\psi_T \mathrm{uly}}{\cos\phi_T \cos\varepsilon_L}\right) - \frac{\sin\varepsilon_L \cos\theta_T}{\cos\phi_T \cos^2\varepsilon_L}\left(\sin\psi_T \mathrm{ulx} - \cos\psi_T \mathrm{uly}\right)^2$$

$$\frac{\partial \phi_T}{\partial \theta_T} = \frac{\tan\varepsilon_L}{\cos\phi_T \cos^2\varepsilon_L}\left(\sin\psi_T \mathrm{ulx} - \cos\psi_T \mathrm{uly}\right)\left(\sin\theta_T\left(\cos\psi_T \mathrm{ulx} + \sin\psi_T \mathrm{uly}\right) + \cos\psi_T \mathrm{ulz}\right)$$

Figure 19. Derivatives of triangle roll

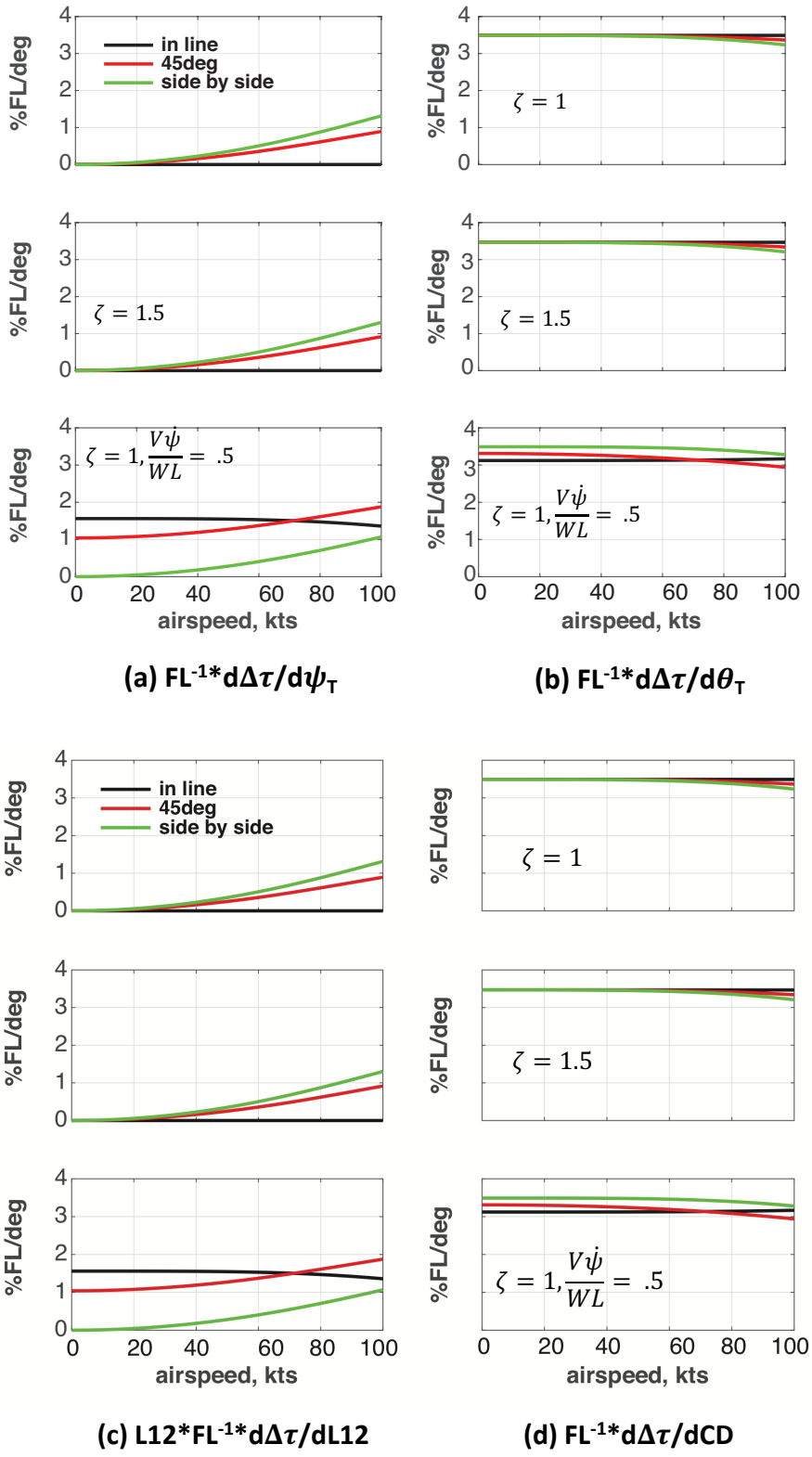

Figure 20. Effects of unequal loading and steady turns on sensitivities

APPENDIX C. UH-60A AIRFRAME AERODYNAMICS

The objective is to generate a table of airframe aerodynamics as a function of angle of attack (aoa) and airspeed that is approximately valid for the trimmed helicopter. The variation with sideslip angle is neglected since helicopter sideslip can be assumed to be maintained at/near zero in quasi-steady flight.

The table of airframe aerodynamics is based on the GenHel model of the UH-60A given in [20], [21], [22]. Reference 22 indicates that GenHel trims were validated against flight data taken every 10 kts from 0 to 160 kts. The trim code was modified to allow the addition of a hook force vector that could be specified by the user, both magnitude and direction. At airspeeds from hover to 120 kts, the direction of the hook force vector was varied within the helicopter X-Z plane sufficiently to get trim aoa in the range of -20 to 20 deg. Trims were calculated for a 16000lb UH-60A carrying a 6000 lb load every 10kts from 0 to 120kts. These data were then interpolated to a common aoa grid. The airframe aerodynamics depend on attitude and airspeed and not on details of helicopter weight and hook force except for some secondary dependence on thrust magnitude. The trim data for this work was provided in [23].

Airframe aerodynamics in the GenHel model are made up of contributions from the fuselage and the horizontal and vertical tails and include the effects of the main rotor downwash. Tail rotor side-wash is present but neglected in the current calculations consistent with omitting the tail rotor thrust in the force balance equation for the simplified helicopter model. The components of the airframe aerodynamics are shown in Fig. 21. Figure 21(a) shows the fuselage aerodynamics. Drag is in the range of 800 to 1200 lbs at 100kts and lift is in the range of -1800 to 1000lbs at 100kts. Figure 21(b) shows the horizontal tail contribution. The horizontal tail of the UH-60A is all-moving (stabilator). The stabilator angle is set automatically as a function of airspeed from 40 deg at hover to about 6 deg at 100kts. Drag is minor for $|aoa| < 10$ deg and larger at higher aoa. Lift is more significant since the horizontal tail is a lifting surface and, at high speeds and high aoa, its lift is larger in magnitude than fuselage lift. The vertical tail contribution to the aerodynamics (Fig. 21(c)) is negligible in this context.

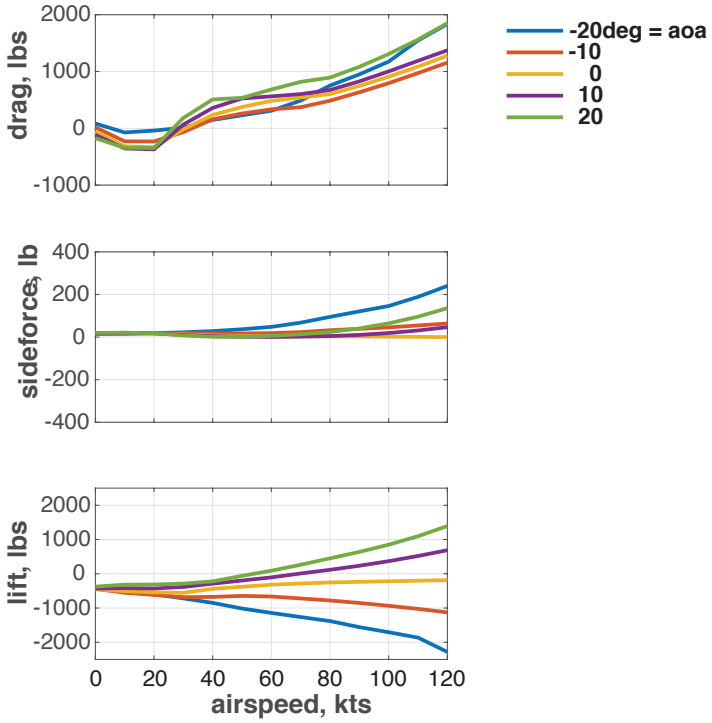

(a) fuselage

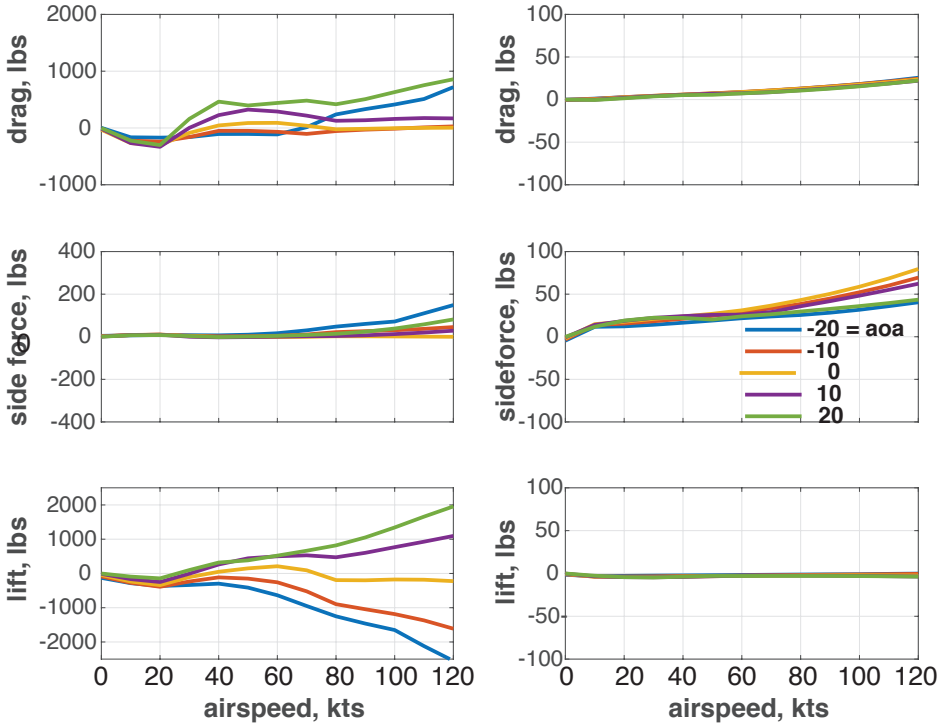

(b) horizontal tail

(c) vertical tail

Figure 21. Fuselage and empennage aerodynamics

The airframe aerodynamics are the sum of these functions and were previously given in Fig. 11 in the text. Figure 11 is repeated here for convenience. Drag reaches 1000 to 2000 lbs at 100 kts depending on aoa, and lift is in the range of -3500 to 2000 lbs at 100kts.

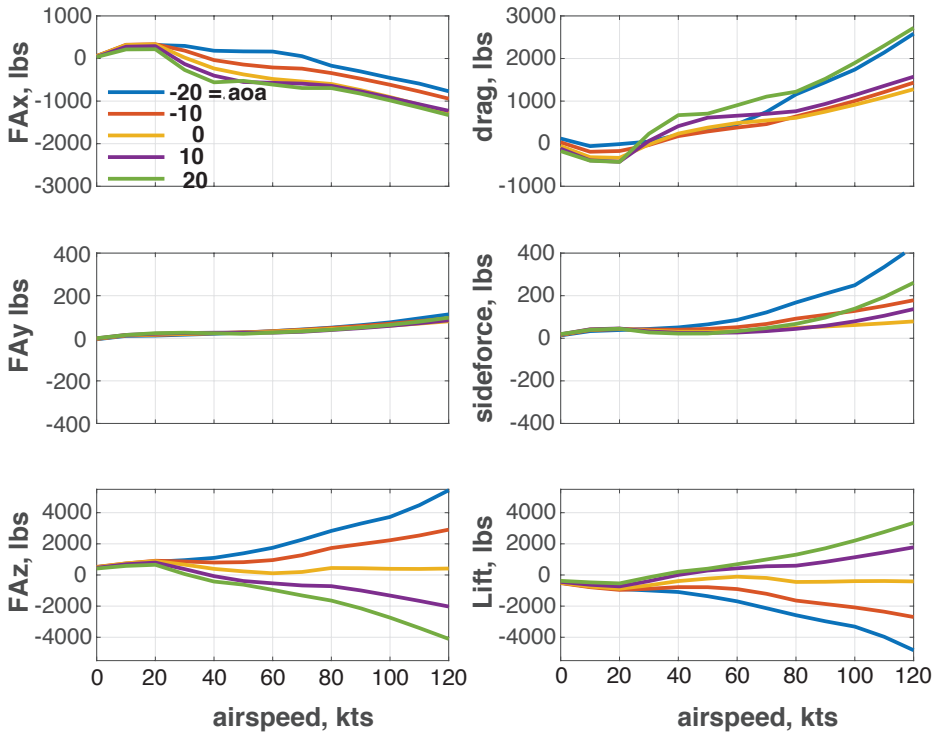

Figure 11. Airframe aerodynamic forces (sideslip = 0)

The results given here are in lbs of force corresponding to sea level standard day atmospheric conditions, and can be scaled by dynamic pressure to general atmospheric conditions and altitudes.

Numerical values for the body axes components are given in Table 2.

Table 2. Airframe aerodynamic forces: sideslip = 0, body axes components

(a) X force, lbs

		angle of attack, deg										
		−20	−16	−12	−8	−4	0	4	8	12	16	20
	0	57	58	59	59	59	57	50	42	37	34	35
	10	306	315	321	322	320	317	305	287	265	240	213
	20	317	326	333	336	336	333	319	300	278	249	218
	30	296	262	214	153	88	21	−44	−102	−156	−212	−268
V	40	182	107	9	−81	−160	−234	−302	−367	−437	−508	−559
(kts)	50	167	33	−90	−192	−280	−373	−451	−518	−555	−548	−524
	60	163	−2	−152	−268	−383	−480	−530	−559	−586	−617	−612
	70	54	−71	−174	−310	−444	−539	−574	−585	−611	−666	−693
	80	−169	−255	−316	−387	−500	−597	−639	−644	−646	−672	−694
	90	−303	−386	−444	−524	−648	−741	−776	−777	−775	−793	−824
	100	−454	−520	−577	−673	−814	−905	−933	−926	−917	−943	−983
	110	−589	−651	−717	−831	−989	−1083	−1108	−1091	−1056	−1101	−1152

(b) Y force, lbs

		−20	−16	−12	−8	−4	0	4	8	12	16	20
	0	−4	−4	−3	−3	−2	−1	−1	−0	−0	0	0
	10	11	12	12	13	14	14	15	15	15	15	15
	20	12	13	15	16	16	17	19	20	21	23	23
	30	16	18	19	19	20	21	22	24	25	25	26
V	40	21	22	23	23	23	24	25	26	25	24	23
(kts)	50	26	27	27	27	27	27	27	27	24	21	20
	60	33	33	33	32	32	31	30	28	25	25	26
	70	41	41	40	39	37	37	34	31	30	32	32
	80	50	49	49	47	45	43	41	38	39	41	40
	90	61	60	58	56	53	51	48	47	49	50	50
	100	74	73	70	66	62	59	56	56	60	61	62
	110	93	88	83	77	72	68	66	68	72	75	77

(c) Z force, lbs

		−20	−16	−12	−8	−4	0	4	8	12	16	20
	0	510	518	521	516	508	496	482	466	450	433	414
	10	681	709	733	746	750	746	729	703	669	628	582
	20	850	880	905	918	912	888	855	817	771	717	655
	30	952	927	891	838	763	664	550	434	317	196	59
V	40	1097	1019	878	717	553	391	225	38	−173	−320	−421
(kts)	50	1390	1175	942	702	488	231	−53	−291	−438	−512	−620
	60	1746	1431	1099	813	474	109	−223	−450	−620	−784	−957
	70	2264	1841	1463	1072	622	191	−189	−521	−819	−1090	−1316
	80	2831	2348	1929	1479	961	448	−29	−486	−938	−1334	−1645
	90	3298	2744	2238	1666	1040	435	−141	−708	−1259	−1736	−2140
	100	3726	3155	2561	1849	1106	395	−294	−982	−1647	−2214	−2738
	110	4480	3727	2969	2085	1217	387	−429	−1257	−2066	−2740	−3404

REFERENCES

1. Sheridan, P. F.: "Feasibility Study for Multiple Helicopter Heavy Lift Systems", Report R-136, Vertol Aircraft Corp., Philadelphia, PA, October 1957

2. Meek, T., Chesley, G. B.: "Twin Helicopter Lift System Study and Feasibility", Demonstration. Sikorsky engineering report SER-64323, Sikorsky Aircraft Co, Stratford, Conn., December 1970

3. Meir, W. H., Olson, J. R.: "Efficient Sizing of a Cargo Rotorcraft", *Journal of Aircraft*, Vol 23, No 6, 1987

4. Carter, E. R.: "Implication of Heavy Lift Helicopter Size Effect Trends and Multi-lift Options for Filling The Need", Proceedings of the 8th European Rotorcraft Forum, Aix-en-Provence, France, September 1982

5. Cicolani, L. S., Kanning, G.: "General Equilibrium Characteristics of a Dual-Lift Helicopter System", NASA TP 2615, July, 1986

6. Curtiss, H. C., Warburton, F. W.: "Stability and Control of The Twin Lift Helicopter System", *Journal of the American Helicopter Society*, April, 1985

7. Cicolani, L. S., Kanning, G.: "Equations of Motion Of Slung Load Systems Including Multilift Systems", NASA TP 3280, November 1992

8. Cicolani, L. S., Kanning, G., Synnestvedt, R.: "Simulation of the Dynamics of Slung Load Systems.", *Journal of the American Helicopter Society*, April, 1985

9. Mittal, M.: "Modeling and Control of a Helicopter Twin Lift System", PHD dissertation, Georgia Institute of Technology, November 1991

10. Menon, P. K. A., Prasad, J. V. R., and Schrage, D. P., "Nonlinear Control of a Twin-Lift Helicopter Configuration," *Journal of Guidance, Control and Dynamics*, Vol. 14, (6), November 1991, pp. 1287–1293.

11. Mittal, M., Prasad, J. V. R.: "Three-Dimensional Modeling and Control of a Helicopter Twin Lift System", *Journal of Guidance, Control and Dynamics*, Vol 16(1), pp 86-95, 1993

12. Bernard, M., Kondak, K.: "Generic Slung Load Transportation System Using Small Size Helicopters", 2009 IEEE International Conference on Robotics and Automation. Kobe, Japan, May 12-17, 2009

13. Bernard, M., Kondak, K., Maza, I., Ollero,A.: "Autonomous Transportation And Deployment With Aerial Robots For Search And Rescue Missions", *Journal of Field Robotics*, Vol 28, No. 6, October 2011

14. Enciu, J., Horn, J. F., Langelaan, J.: "Formation Control of a Rotorcraft Multi-Lift System", *Journal of the American Helicopter Society*. October, 2017

15. Enciu, J., Horn, J. F., "Flight Performance Optimization of a Multi-Lift Rotorcraft Formation", *Journal of Aircraft*, January 2017

16. Berrios, M. G., Tischler, M. B., Cicolani, L. S., Powell, J. D.: "Stability, Control and Simulation of a Dual Lift System Using Autonomous R-MAX Helicopters", Proceedings of the 70th Annual Forum of the American Helicopter Society, Montreal, Quebec, Canada, May 20-22, 2014

17. Raz, R., Fogel, O., Rosen, A., Berrios, M. G., Cicolani, L. S.: "Using Wind Tunnel Tests to Investigate Dual Lift Trim, Maneuvers, Stability and Control", Proceedings of the 73rd Annual Forum of the American Helicopter Society, Fort Worth, Texas, May 9-11, 2017

18. Berrios, M.G., Takahashi, M.D., Whalley, M.S., Schulein, G.J., Cicolani, L.S., and Powell, J.D. "Load Distribution Control for a Dual Lift System using RMAX UAVs with Flight Test Results," Proceedings of the 74th Annual Forum of the American helicopter Society, Phoenix, Az, May 14-17, 2018

19. Takahashi, M.D., Whalley, M.S., Schulein, and G.J., Berrios, M.G., "Autonomous Rotorcraft Flight Control for Dual-Ship Sling-Load Operations," Proceedings of the 74th Annual Forum of the American helicopter Society, Phoenix, Az, May 14-17, 2018

20. Howlett, J. J.: "UH-60A Black Hawk Engineering Simulation Program: Vol I, Mathematical Model", NASA CR-166309, December, 1981

21. Kaplita, T. T.: "UH-60 Black Hawk Engineering Simulation Model Validation and Proposed Modifications", NASA CR 177360, July, 1985

22. Ballin, M. G.: "Validation of a Real-Time Engineering Simulation of the UH-60A Helicopter", NASA TM 88360, Febuary, 1987

23. Tobias, E.: "GenHel Trim files from Code Modified to Include Hook Forces," Internal communication, March 2015